

Structure and reactions in Fermionic Molecular Dynamics



Thomas Neff

**YIPQS Long-term workshop
“Computational Advances in
Nuclear and Hadron Physics”**

Yukawa Institute, Kyoto, Japan

October 13, 2015



Overview



Realistic Effective Nucleon-Nucleon interaction:
Unitary Correlation Operator Method

Many-Body Approach:
Fermionic Molecular Dynamics

Applications:

${}^3\text{He}(\alpha, \gamma){}^7\text{Be}$ Radiative Capture Reaction

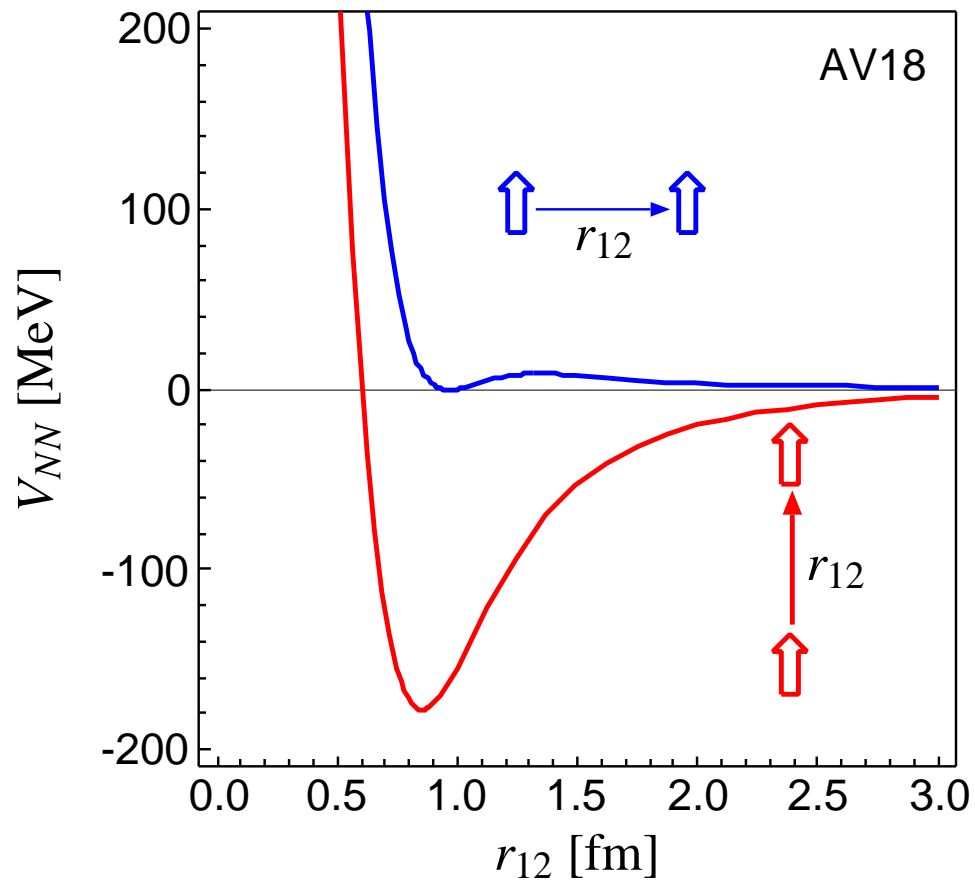
${}^{12}\text{C}$ in the Microscopic Cluster Model

${}^{12}\text{C}$ in Fermionic Molecular Dynamics

Nuclear Force

Argonne V18 (T=0)

spins aligned parallel or perpendicular to the relative distance vector



- strong repulsive core: nucleons can not get closer than ≈ 0.5 fm

➔ **central correlations**

- strong dependence on the orientation of the spins due to the tensor force

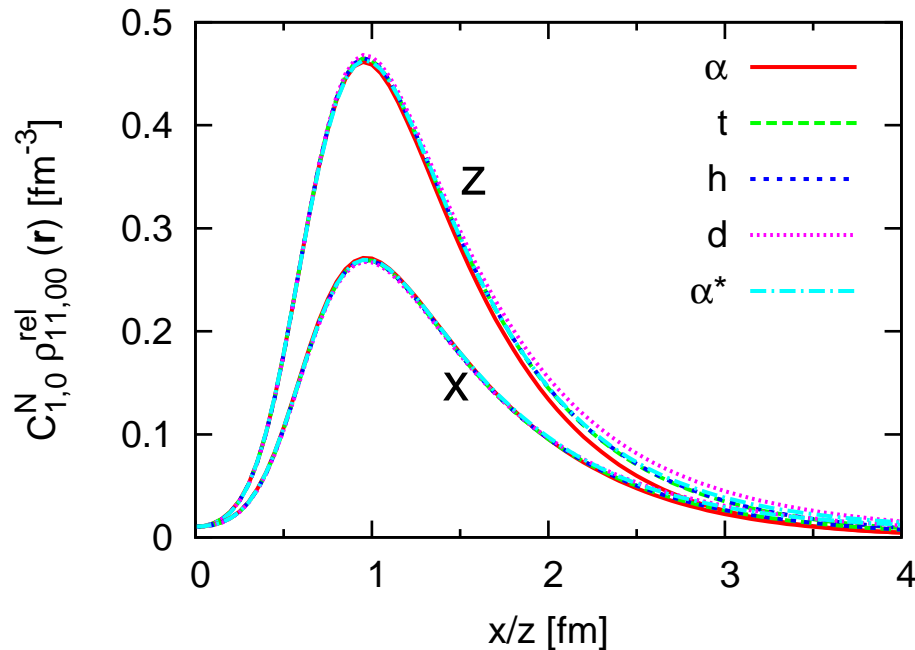
➔ **tensor correlations**

the nuclear force will induce **strong short-range correlations** in the nuclear wave function

- Universality of short-range correlations
- **Two-body densities in $A = 2, 3, 4$ Nuclei — AV8'**

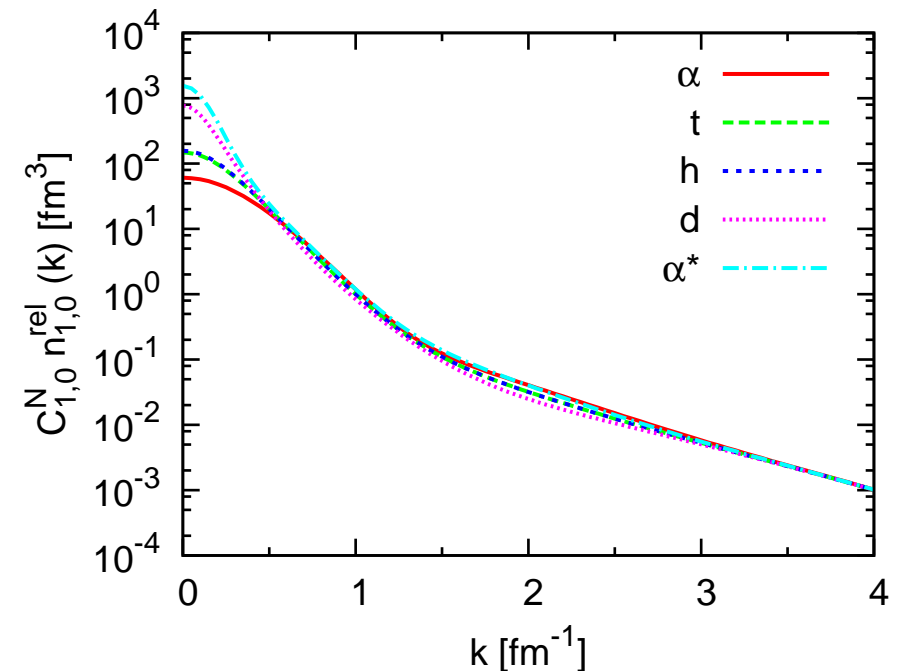
coordinate space

$S = 1, M_S = 1, T = 0$



momentum space

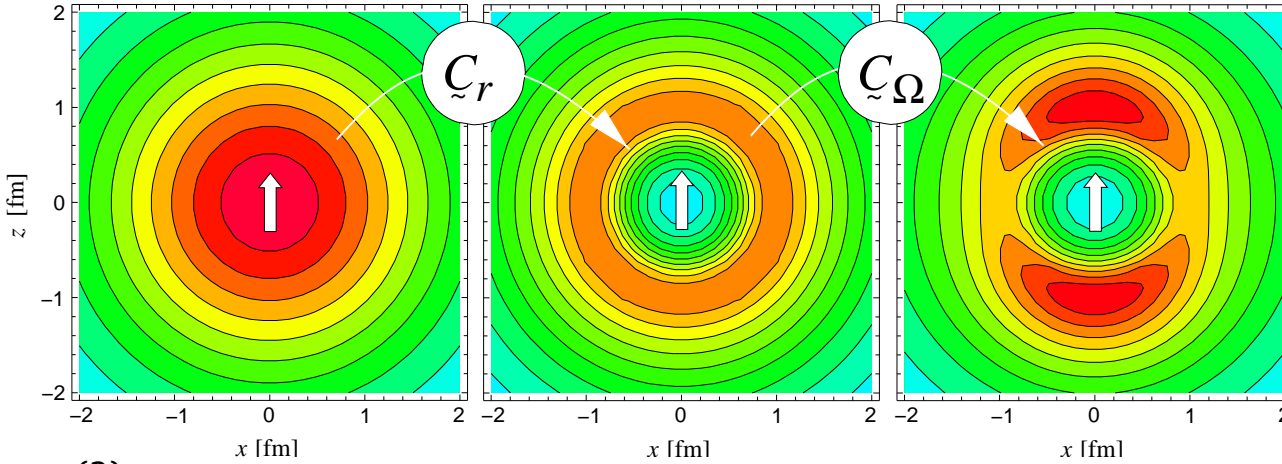
$S = 1, T = 0$



- normalize two-body density in coordinate space at $r=1.0$ fm
- normalized two-body densities in coordinate space are identical at short distances for all nuclei
- use the **same** normalization factor in momentum space – high momentum tails agree for all nuclei

Correlations and Energies

two-body densities



$$\rho_{S,T}^{(2)}(\mathbf{r}_1 - \mathbf{r}_2) \quad S = 1, M_S = 1, T = 0$$

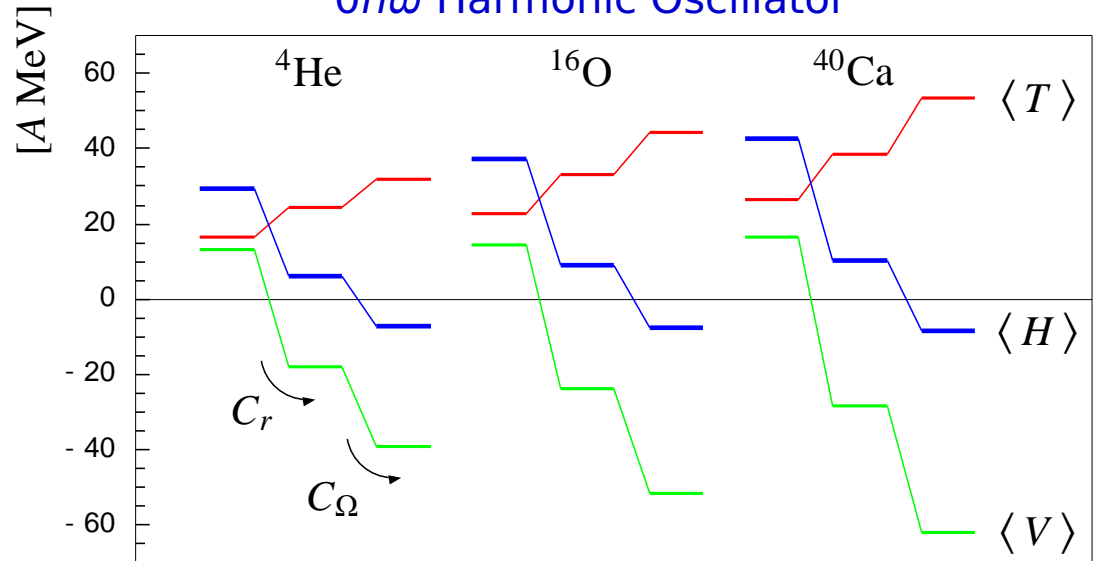
central correlator C_r
shifts density out of the repulsive core

tensor correlator C_Ω
aligns density with spin orientation

both central and tensor correlations are essential for binding

energies

$0\hbar\omega$ Harmonic Oscillator



Neff and Feldmeier, Nucl. Phys. **A713** (2003) 311

Roth, Neff, Feldmeier, Prog. Part. Nucl. Phys. **65**, (2010) 50

Fermionic

Slater determinant

$$|Q\rangle = \mathcal{A}\left(|q_1\rangle \otimes \cdots \otimes |q_A\rangle\right)$$

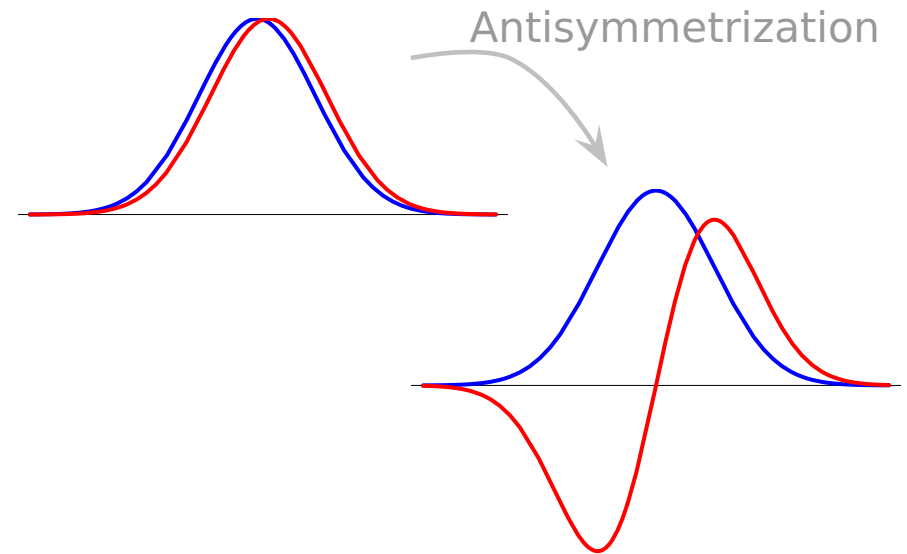
- antisymmetrized A-body state

Molecular

single-particle states

$$\langle \mathbf{x} | q \rangle = \sum_i c_i \exp\left\{-\frac{(\mathbf{x} - \mathbf{b}_i)^2}{2a_i}\right\} \otimes |\chi_i^\uparrow, \chi_i^\downarrow\rangle \otimes |\xi\rangle$$

- Gaussian wave-packets in phase-space (complex parameter \mathbf{b}_i encodes mean position and mean momentum), spin is free, isospin is fixed
- width a_i is an independent variational parameter for each wave packet
- use one or two wave packets for each single particle state



FMD basis contains
HO shell model and
microscopic cluster model
as limiting cases

Evaluation of Matrix Elements

➔ non-orthogonal basis, use inverse overlap matrix

One-Body Operators

$$\frac{\langle Q | \tilde{T}^{[1]} | Q \rangle}{\langle Q | Q \rangle} = \sum_{k,l}^A \langle q_k | \tilde{T}^{[1]} | q_l \rangle o_{lk}$$

Two-Body Operators

$$\frac{\langle Q | \tilde{V}^{[2]} | Q \rangle}{\langle Q | Q \rangle} = \frac{1}{2} \sum_{k,l,m,n}^A \langle q_k, q_l | \tilde{V}^{[2]} | q_m, q_n \rangle (o_{mk} o_{nl} - o_{ml} o_{nk})$$

$$o = n^{-1} = \left(\langle q_i | q_j \rangle \right)^{-1}$$

Operator Representation of V_{UCOM}

$$\tilde{\zeta}^\dagger (\tilde{T} + \tilde{V}) \tilde{\zeta} = \tilde{T}$$

$$+ \sum_{ST} \hat{V}_c^{ST}(r) + \frac{1}{2} (p_r^2 \hat{V}_{p^2}^{ST}(r) + \hat{V}_{p^2}^{ST}(r) p_r^2) + \hat{V}_{l^2}^{ST}(r) \mathbf{l}^2$$

one-body kinetic energy

central potentials

$$+ \sum_T \hat{V}_{ls}^T(r) \mathbf{l} \cdot \mathbf{s} + \hat{V}_{l^2ls}^T(r) \mathbf{l}^2 \mathbf{l} \cdot \mathbf{s}$$

spin-orbit potentials

$$+ \sum_T \hat{V}_t^T(r) \mathcal{S}_{12}(\mathbf{r}, \mathbf{r}) + \hat{V}_{trp_\Omega}^T(r) p_r \mathcal{S}_{12}(\mathbf{r}, \mathbf{p}_\Omega) + \hat{V}_{tll}^T(r) \mathcal{S}_{12}(\mathbf{l}, \mathbf{l}) +$$

$$\hat{V}_{tp_\Omega p_\Omega}^T(r) \mathcal{S}_{12}(\mathbf{p}_\Omega, \mathbf{p}_\Omega) + \hat{V}_{l^2tp_\Omega p_\Omega}^T(r) \mathbf{l}^2 \mathcal{S}_{12}(\mathbf{p}_\Omega, \mathbf{p}_\Omega)$$

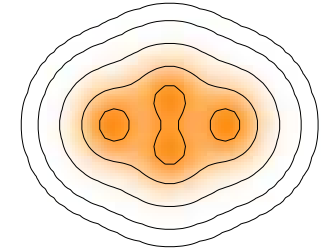
tensor potentials

bulk of tensor force mapped onto central part of correlated interaction
 tensor correlations also change the spin-orbit part of the interaction

Symmetries and Projection

Breaking of symmetries

- Slater determinants $|Q\rangle$ may break symmetries of the Hamiltonian with respect to parity, rotations and translations



Projection

- Restore symmetries by projection

$$\tilde{P}^\pi = \frac{1}{2}(1 + \pi\Pi), \quad \tilde{P}_{MK}^J = \frac{2J+1}{8\pi^2} \int d^3\Omega D_{MK}^{J*}(\Omega) \tilde{R}(\Omega), \quad \tilde{P}^{\mathbf{P}} = \frac{1}{(2\pi)^3} \int d^3X \exp\{-i(\tilde{\mathbf{P}} - \mathbf{P}) \cdot \mathbf{X}\}$$

Multiconfiguration Mixing

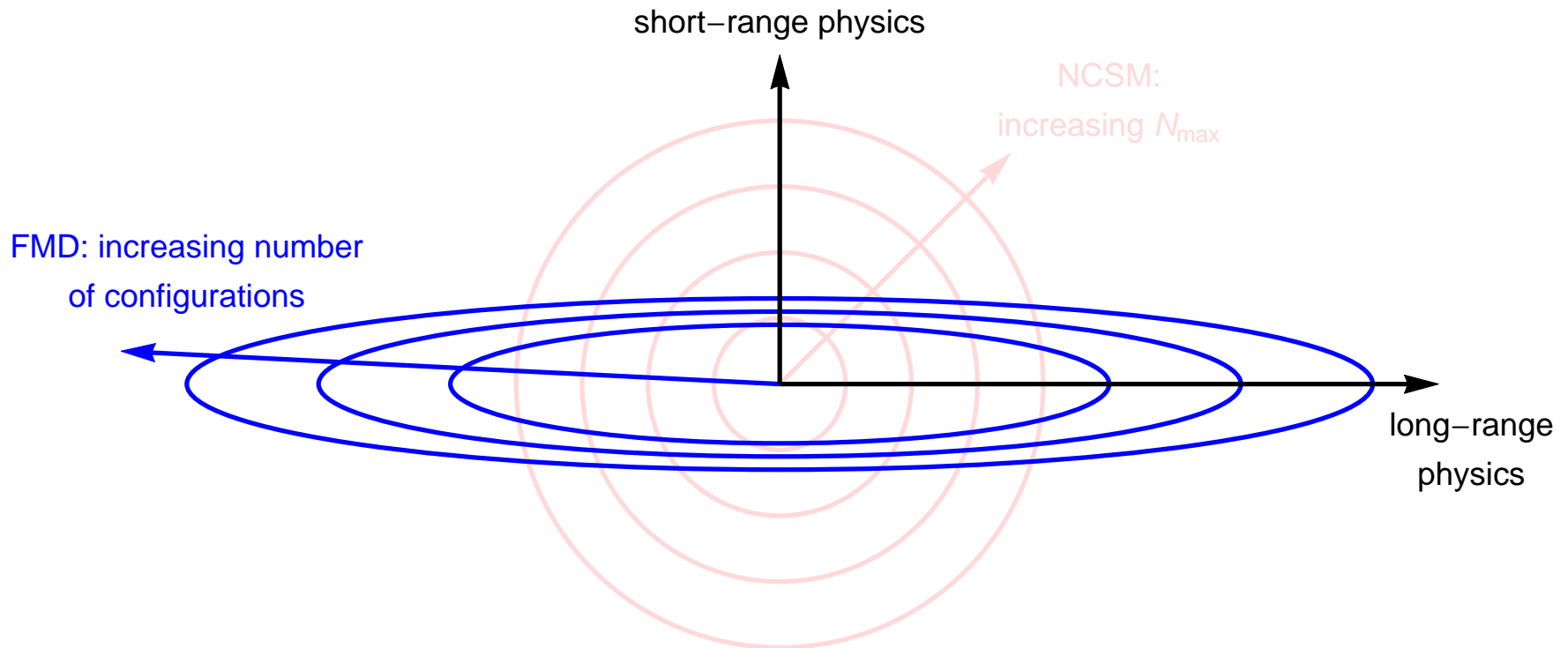
- diagonalize** Hamiltonian in a set of projected intrinsic states $\{|Q^{(a)}\rangle, a = 1, \dots, N\}$

$$|\Psi; J^\pi M \alpha\rangle = \sum_{K\alpha} \tilde{P}^\pi \tilde{P}_{MK}^J \tilde{P}^{\mathbf{P}=0} |Q^{(a)}\rangle c_{K\alpha}^\alpha$$

$$\sum_{K'b} \underbrace{\langle Q^{(a)} | \tilde{H} \tilde{P}^\pi \tilde{P}_{KK'}^J \tilde{P}^{\mathbf{P}=0} | Q^{(b)} \rangle}_{\text{Hamiltonian kernel}} c_{K'b}^\alpha = E^{J^\pi \alpha} \sum_{K'b} \underbrace{\langle Q^{(a)} | \tilde{P}^\pi \tilde{P}_{KK'}^J \tilde{P}^{\mathbf{P}=0} | Q^{(b)} \rangle}_{\text{norm kernel}} c_{K'b}^\alpha$$

• FMD

• FMD vs NCSM model spaces



- NCSM allows good description of short-range physics, but long-range behavior suffers from harmonic oscillator asymptotics
- FMD allows to describe long-range physics by superposition of localized cluster configurations, but limited in description of short-range physics

${}^3\text{He}(\alpha, \gamma){}^7\text{Be}$ radiative capture

one of the key reactions in the solar pp-chains



Effective Nucleon-Nucleon interaction:

AV18-UCOM(SRG)

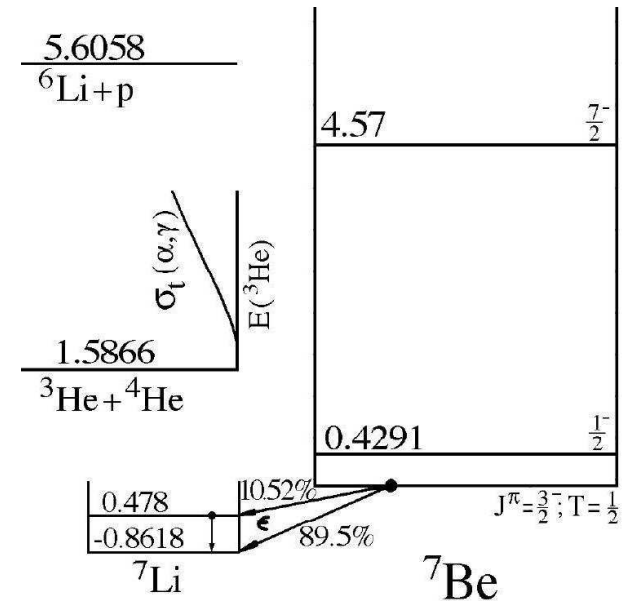
$$\alpha = 0.20 \text{ fm}^4 - \lambda \approx 1.5 \text{ fm}^{-1}$$

Many-Body Approach:

Fermionic Molecular Dynamics

- bound state wave functions
- scattering state wave functions
- electromagnetic transitions matrix elements between scattering and bound states

Neff, Phys. Rev. Lett. 106, 042502 (2011)



${}^3\text{He}(\alpha, \gamma){}^7\text{Be}$

FMD model space

Frozen configurations

- antisymmetrized wave function built with ${}^4\text{He}$ and ${}^3\text{He}$ FMD clusters up to channel radius $a=12$ fm

Polarized configurations

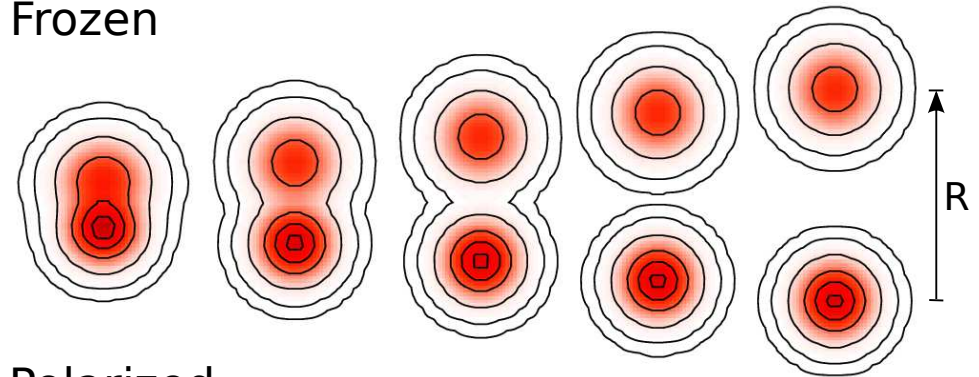
- FMD wave functions obtained by **Variation after Projection** on $1/2^-$, $3/2^-$, $5/2^-$, $7/2^-$ and $1/2^+$, $3/2^+$ and $5/2^+$ combined with radius constraint in the interaction region

Boundary conditions

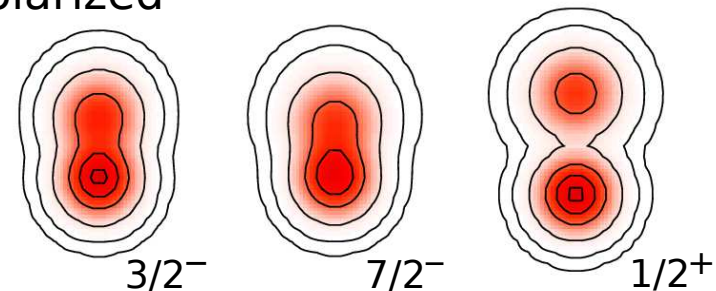
- Match relative motion of clusters at channel radius to Whittaker/Coulomb functions with the **microscopic R-matrix** method of the Brussels group

D. Baye, P.-H. Heenen, P. Descouvemont

Frozen



Polarized



• p -wave Bound and Scattering States

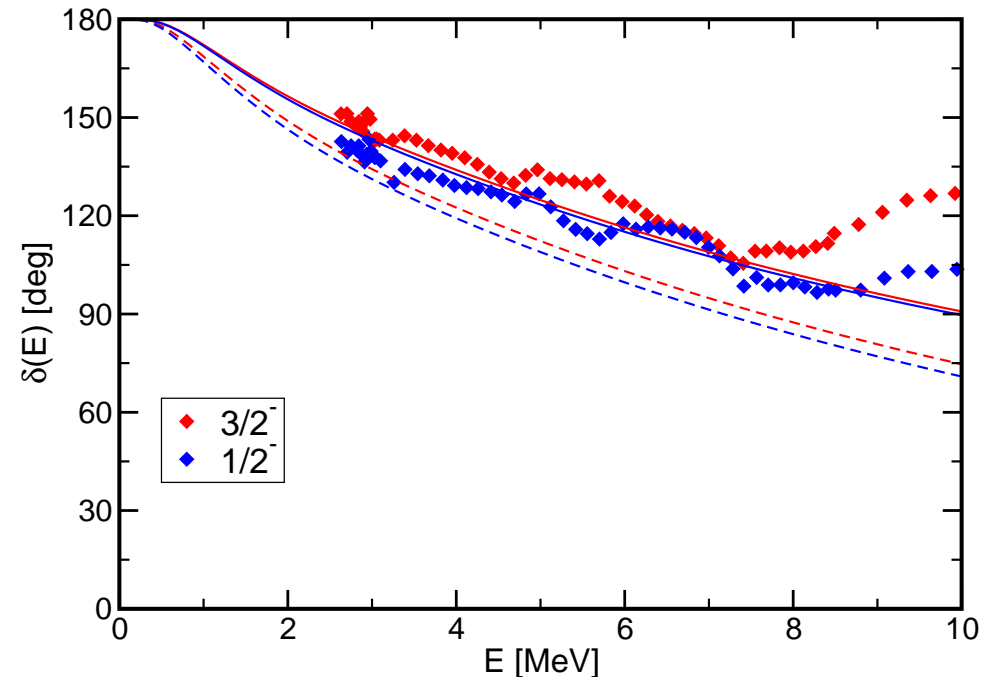
Bound states

		Experiment	FMD
${}^7\text{Be}$	$E_{3/2-}$	-1.59 MeV	-1.49 MeV
	$E_{1/2-}$	-1.15 MeV	-1.31 MeV
	r_{ch}	2.647(17) fm	2.67 fm
	Q	-	-6.83 e fm ²
${}^7\text{Li}$	$E_{3/2-}$	-2.467 MeV	-2.39 MeV
	$E_{1/2-}$	-1.989 MeV	-2.17 MeV
	r_{ch}	2.444(43) fm	2.46 fm
	Q	-4.00(3) e fm ²	-3.91 e fm ²

- centroid of bound state energies well described if polarized configurations included
- tail of wave functions tested by charge radii and quadrupole moments

Phase shift analysis:

Spiger and Tombrello, PR **163**, 964 (1967)

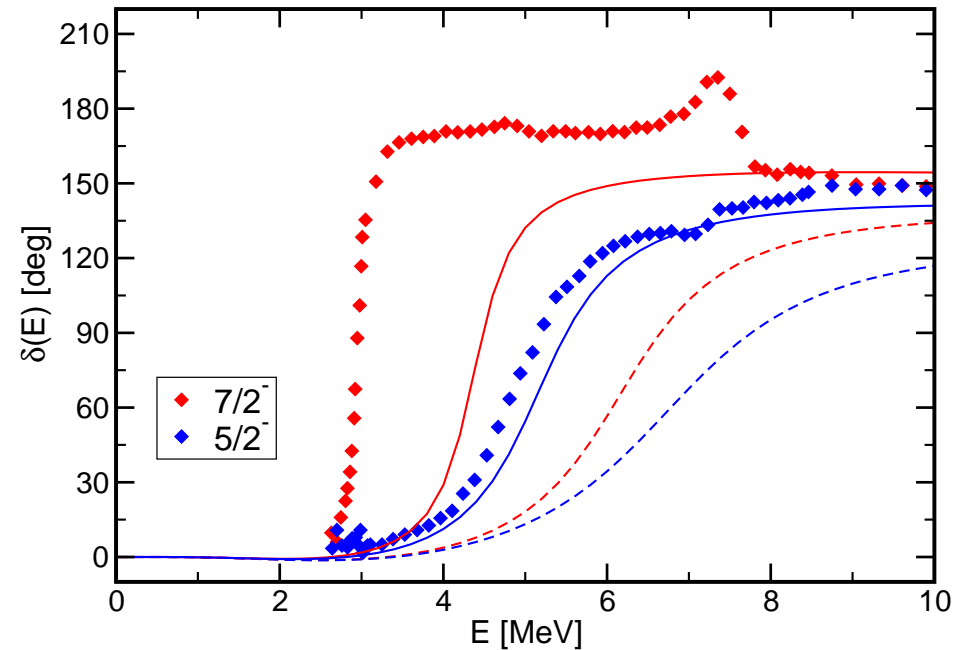
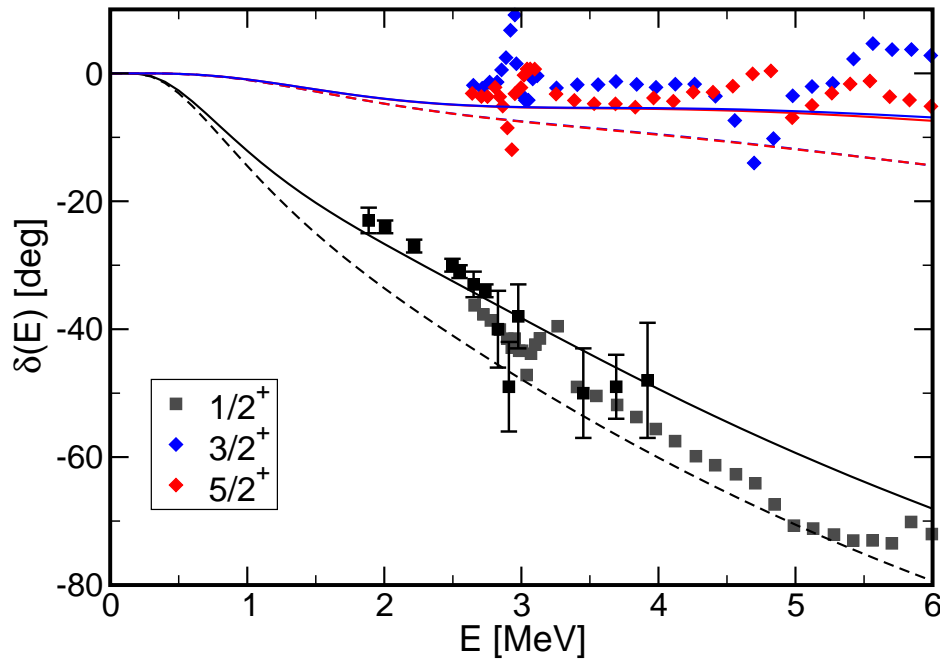


dashed lines – frozen configurations only
solid lines – polarized configurations in interaction region included

- Scattering phase shifts well described, polarization effects important

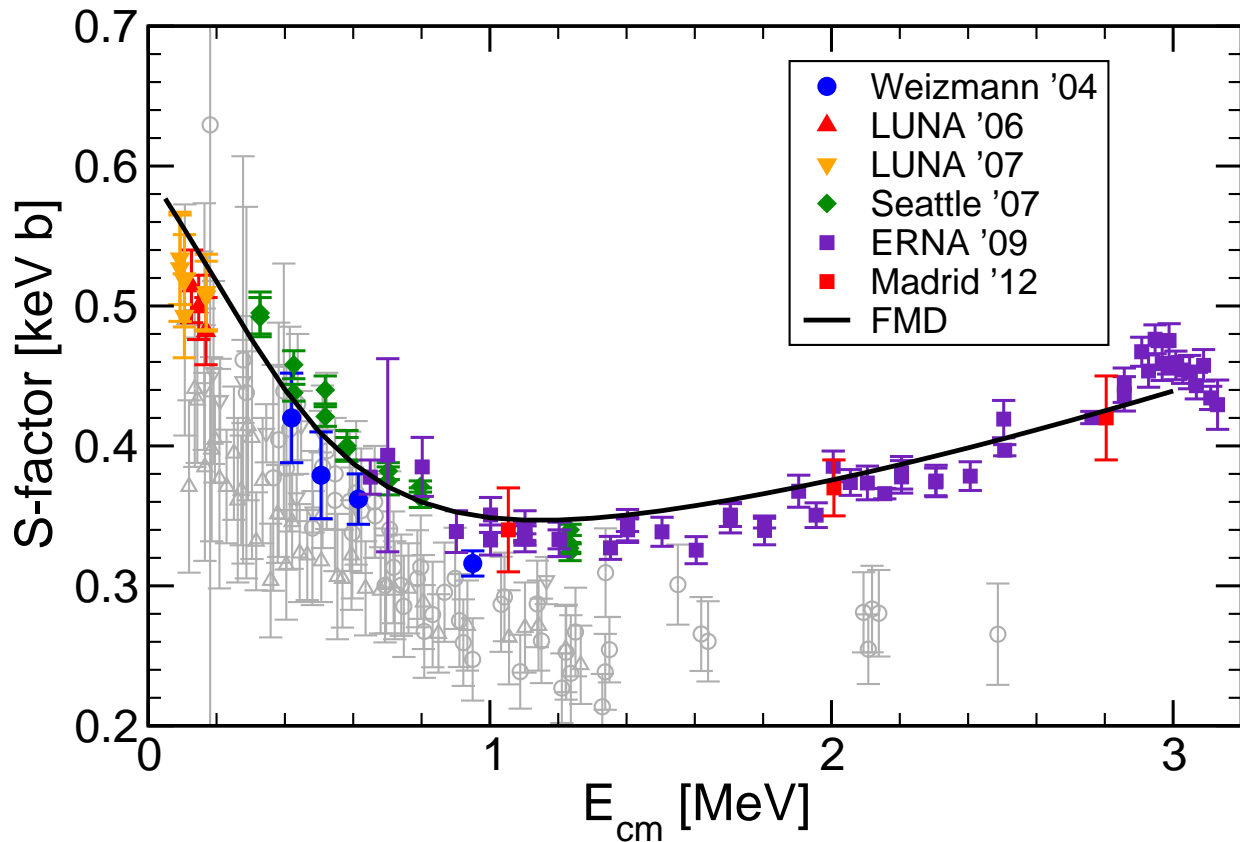
${}^3\text{He}(\alpha, \gamma){}^7\text{Be}$

s -, d - and f -wave Scattering States



dashed lines – frozen configurations only – solid lines – FMD configurations in interaction region included

- polarization effects important
- s - and d -wave scattering phase shifts well described
- f -wave splittings too small, additional spin-orbit strength from three-body forces expected



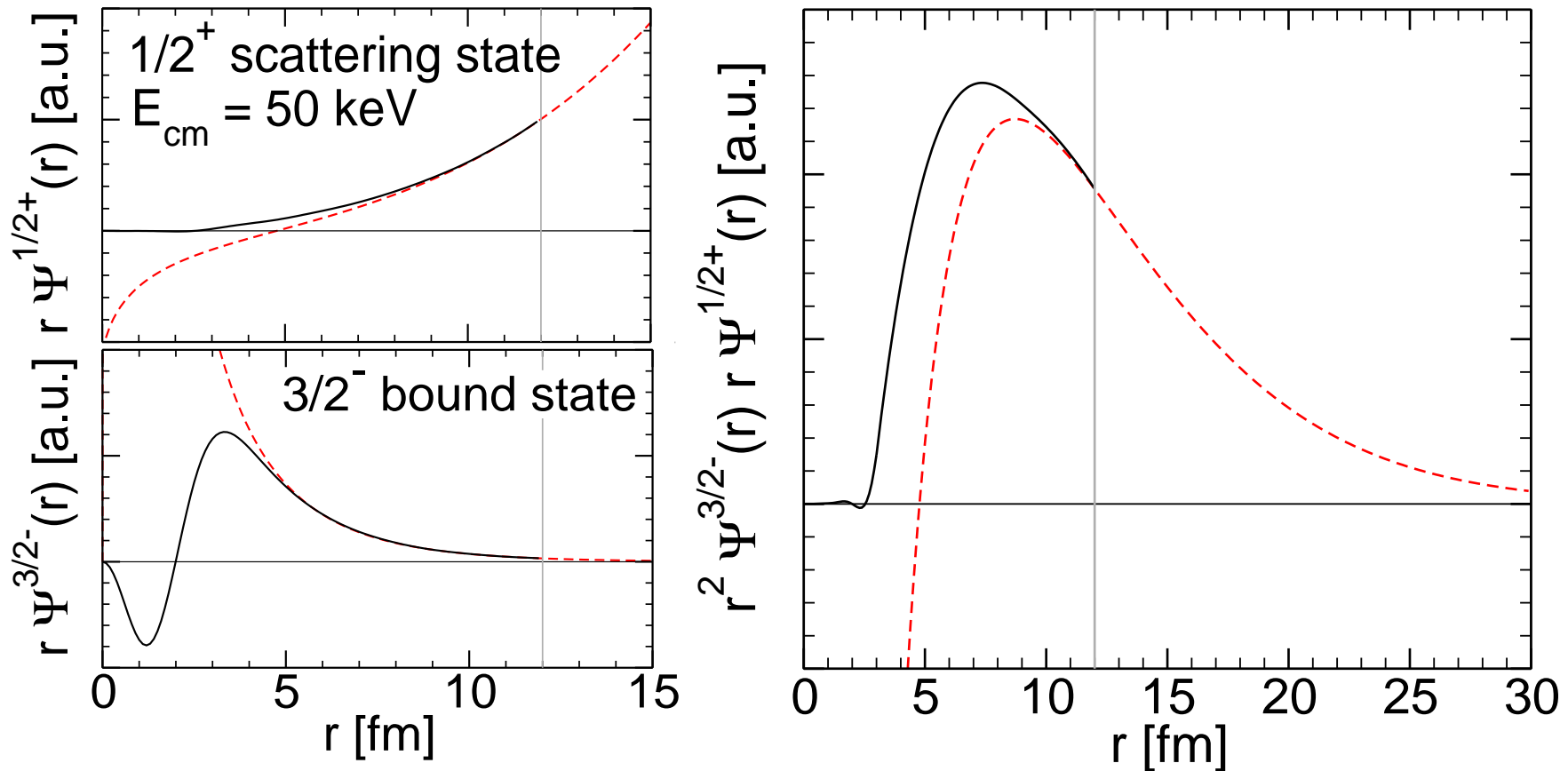
S-factor:

$$S(E) = \sigma(E)E \exp\{2\pi\eta\}$$
$$\eta = \frac{\mu Z_1 Z_2 e^2}{k}$$

Nara Singh *et al.*, PRL **93**, 262503 (2004)
Bemmerer *et al.*, PRL **97**, 122502 (2006)
Confortola *et al.*, PRC **75**, 065803 (2007)
Brown *et al.*, PRC **76**, 055801 (2007)
Di Leva *et al.*, PRL **102**, 232502 (2009)

- dipole transitions from $1/2^+$, $3/2^+$, $5/2^+$ scattering states into $3/2^-$, $1/2^-$ bound states
- ➔ FMD is the only model that describes well the energy dependence and normalization of new high quality data
- ➔ fully microscopic calculation, bound and scattering states are described consistently

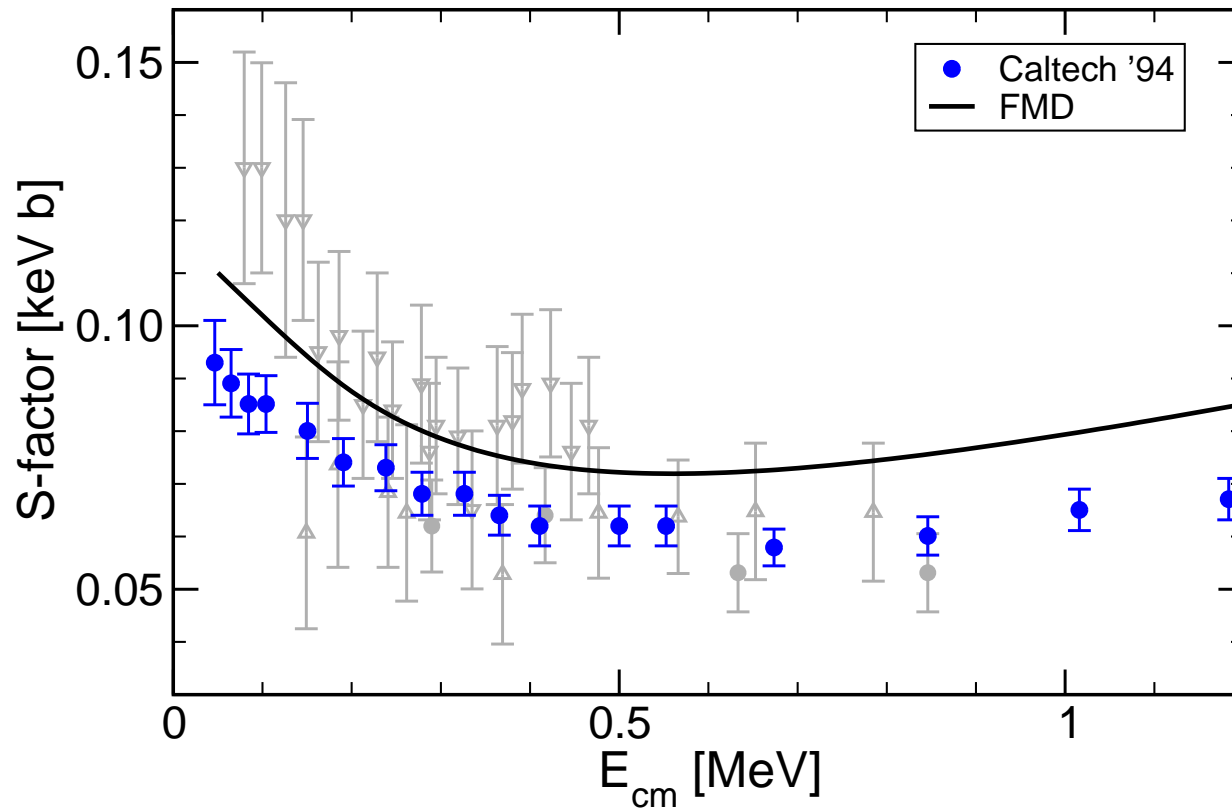
Overlap Functions and Dipole Matrixelements



- Overlap functions from projection on RGM-cluster states
- Coulomb and Whittaker functions matched at channel radius $a=12$ fm
- Dipole matrix elements calculated from overlap functions reproduce full calculation within 2%
- cross section depends significantly on internal part of wave function, description as an “external” capture is too simplified

${}^3\text{H}(\alpha, \gamma){}^7\text{Li}$

S-Factor



S-factor:

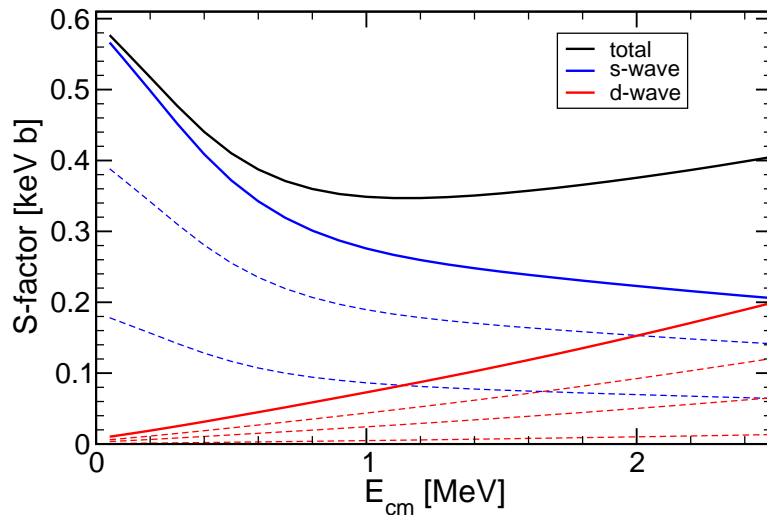
$$S(E) = \sigma(E)E \exp\{2\pi\eta\}$$
$$\eta = \frac{\mu Z_1 Z_2 e^2}{k}$$

Brune *et al.*, PRC **50**, 2205 (1994)

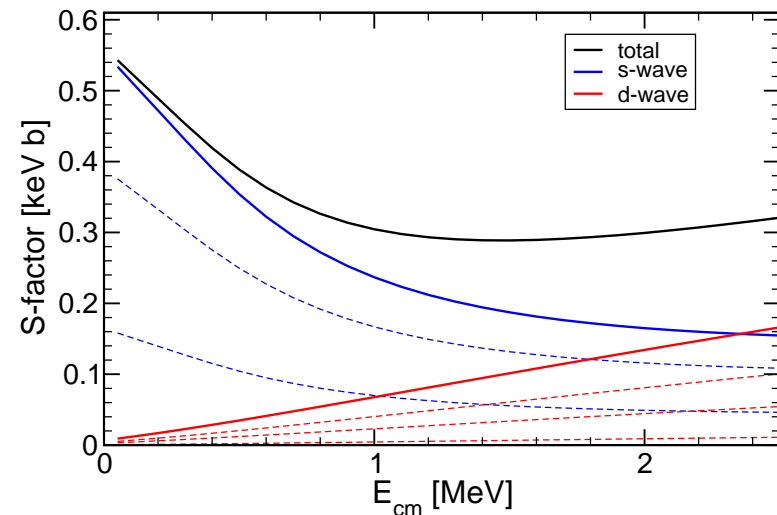
- isospin mirror reaction of ${}^3\text{He}(\alpha, \gamma){}^7\text{Be}$
- ${}^7\text{Li}$ bound state properties and phase shifts well described
- ➔ FMD calculation describes energy dependence of Brune *et al.* data but cross section is larger by about 15%

S-Factor Contributions

FMD

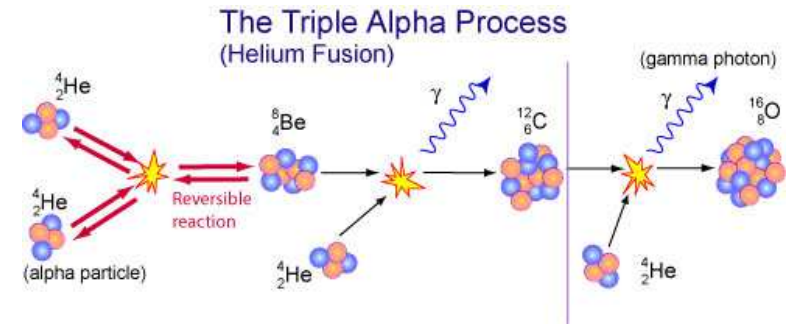


Kajino MHN



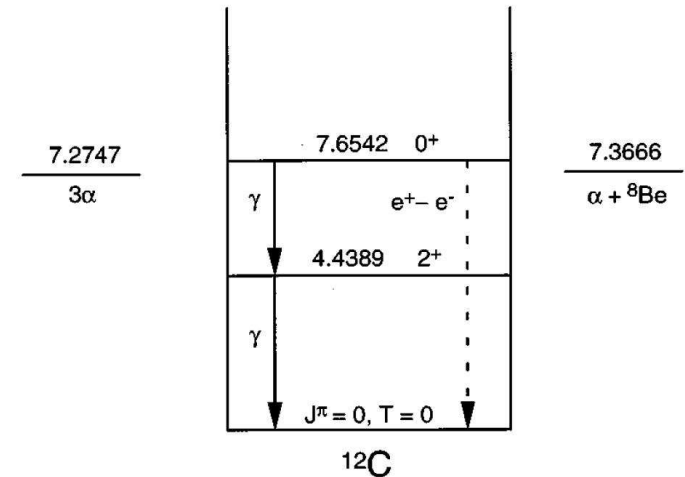
- main difference between FMD and Kajino results is originating in s-wave capture – both in normalization and energy dependence
- difference in normalization related to ground state properties – as seen in charge radius/quadrupole moment
- difference in energy dependence not understood yet – long-range of realistic interaction due to explicit description of pion-exchange ?

Cluster States in ^{12}C



Structure

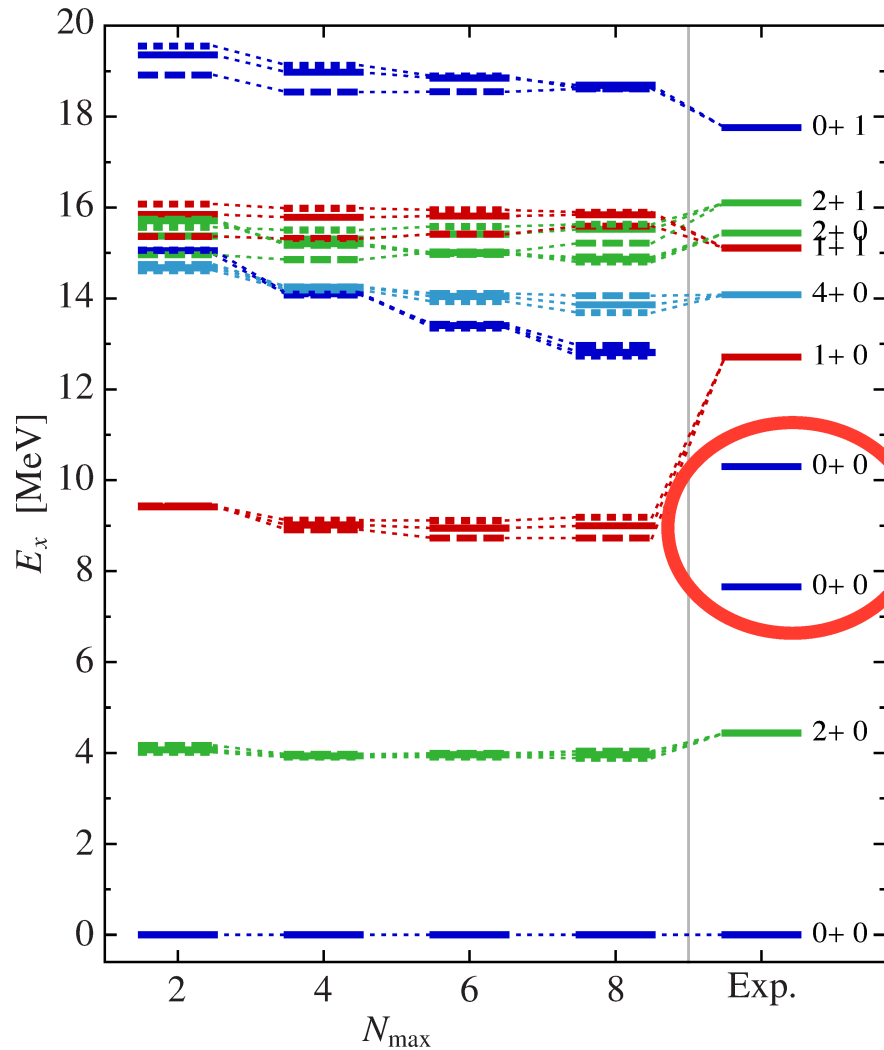
- Is the Hoyle state a pure α -cluster state ?
- Second 2^+ state
Zimmermann *et al.*, Phys. Rev. Lett. 110, 152502 (2013)
- Second 4^+ state
Freer *et al.*, Phys. Rev. C 83, 034314 (2011)
- Other states in the continuum
Fynbo *et al.*, ...



- ➔ Include continuum in the calculation!
- ➔ Compare microscopic α -cluster model and FMD

Neff, Feldmeier, arXiv:1409.3726

^{12}C Cluster States in *ab initio* approaches ?



State of the art NCSM calculation with chiral NN+NNN forces

Hoyle state and other cluster states missing !

Lattice EFT

Green's Function Monte Carlo

Maris, Vary, Calci, Langhammer, Binder, Roth, Phys. Rev. C **90**, 014314 (2014)

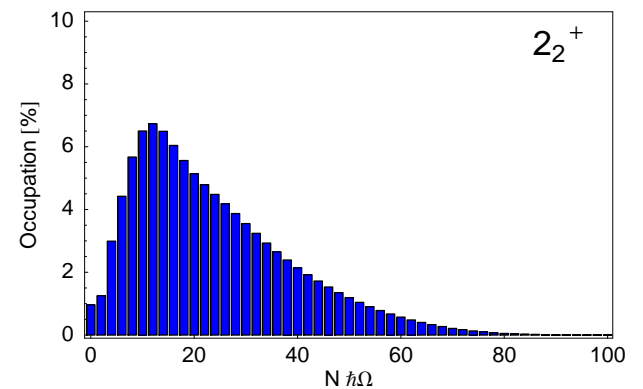
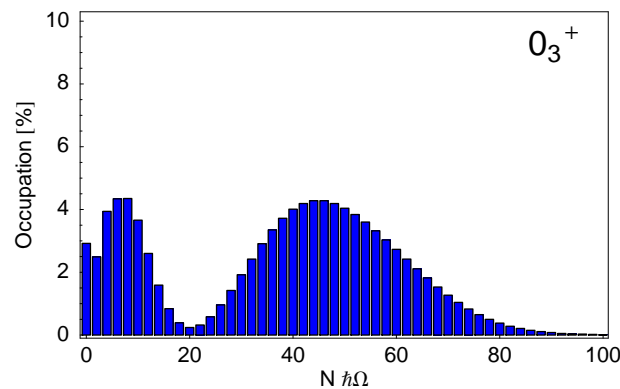
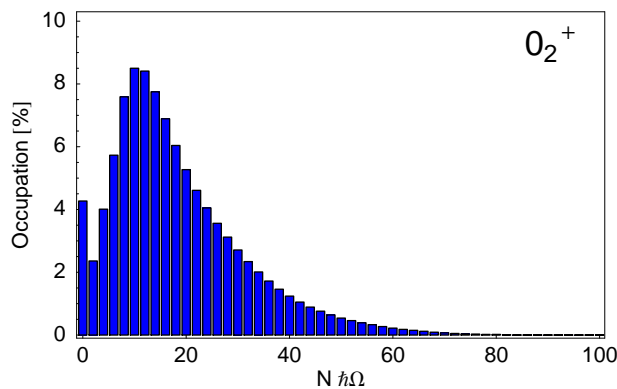
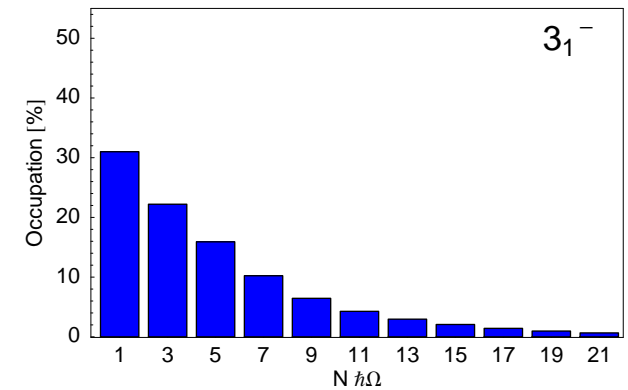
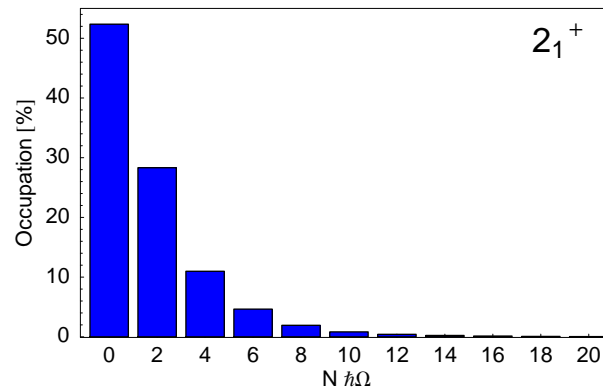
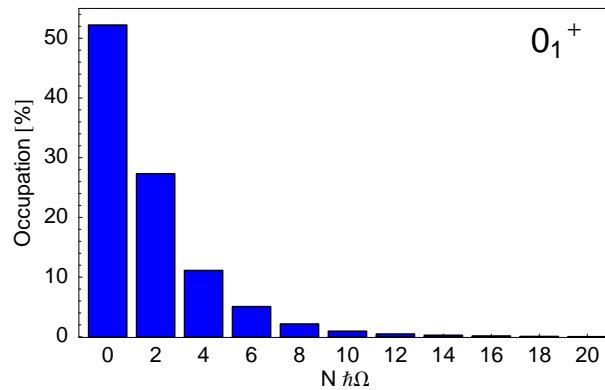
Cluster States in ^{12}C

Harmonic Oscillator $N\hbar\Omega$ Excitations

Y. Suzuki *et al*, Phys. Rev. C **54**, 2073 (1996).

$$\text{Occ}(N) = \langle \Psi | \delta \left(\sum_i (H_i^{HO} / \hbar\Omega - 3/2) - N \right) | \Psi \rangle$$

Cluster Model

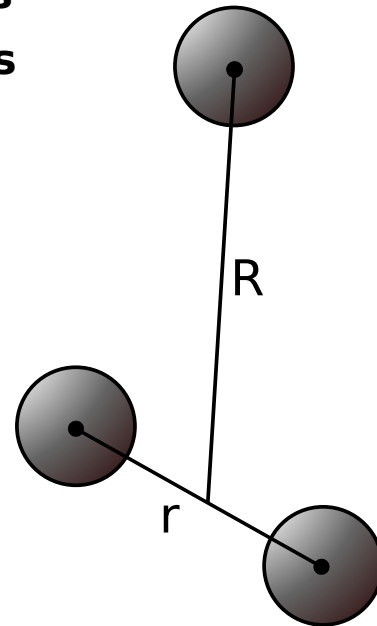


Microscopic α -cluster model



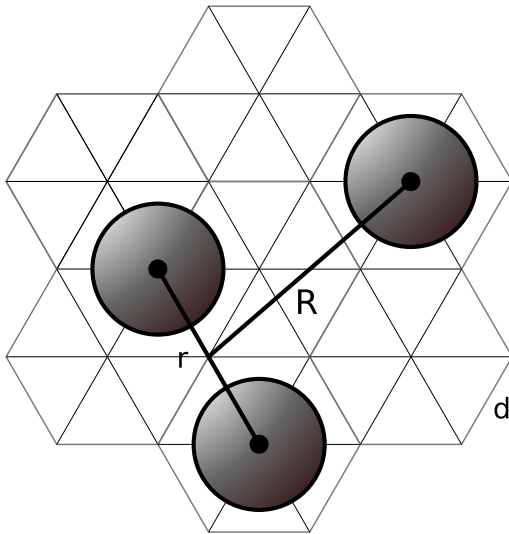
What are the degrees of freedom ?

- ^{12}C is described as a system of three α -particles
 - α -particles are given by HO $(0s)^4$ wave functions
 - wave function is fully antisymmetrized
 - effective nucleon-nucleon interaction adjusted to reproduce α - α and ^{12}C ground state properties
- ➔ include ^8Be - α channels for continuum



Microscopic α -Cluster Model

Model space in internal region



$$\rho^2 = \frac{1}{2} \mathbf{r}^2 + \frac{2}{3} \mathbf{R}^2$$

Hyperradius

Model Space

- include all possible configurations on triangular grid ($d = 1.4$ fm) up to a certain hyperradius ρ
- no restriction on relative angular momenta

Basis States

- Intrinsic states are projected on parity and angular momentum

$$|\Psi_{JMK\pi}^{3\alpha}(\mathbf{R}_1, \mathbf{R}_2, \mathbf{R}_3)\rangle = \underset{\sim}{P}^{\pi} \underset{\sim}{P}_{MK}^J \underset{\sim}{A} \left\{ |\Psi^{4\text{He}}(\mathbf{R}_1)\rangle \otimes |\Psi^{4\text{He}}(\mathbf{R}_2)\rangle \otimes |\Psi^{4\text{He}}(\mathbf{R}_3)\rangle \right\}$$

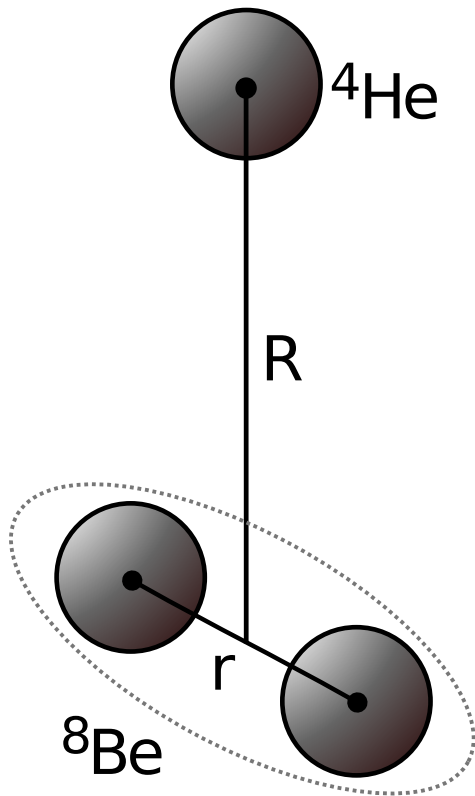
Volkov Interaction

- simple central interaction
- parameters adjusted to give reasonable α binding energy and radius, $\alpha - \alpha$ scattering data, adjusted to reproduce ^{12}C ground state energy

✗ only reasonable for ^4He , ^8Be and ^{12}C nuclei

- Microscopic α -Cluster Model

- Model space in external region



Model Space

- ${}^8\text{Be}$ - ${}^4\text{He}$ cluster configurations with generator coordinate R
- ${}^8\text{Be}$ ground state (0_1^+) and pseudo states (2_1^+ , 0_2^+ , 2_2^+ , 4_1^+) obtained by diagonalizing α - α configurations up to $r = 10$ fm

Basis States

- ${}^{12}\text{C}$ basis states are obtained by **double projection**:
Project first ${}^8\text{Be}$

$$|\Psi_{IK}^{8\text{Be}}\rangle = \sum_i P_{\sim K0}^I \mathcal{A} \left\{ |\Psi^{4\text{He}}(-\frac{r_i}{2}\mathbf{e}_z)\rangle \otimes |\Psi^{4\text{He}}(+\frac{r_i}{2}\mathbf{e}_z)\rangle \right\} c_i^I$$

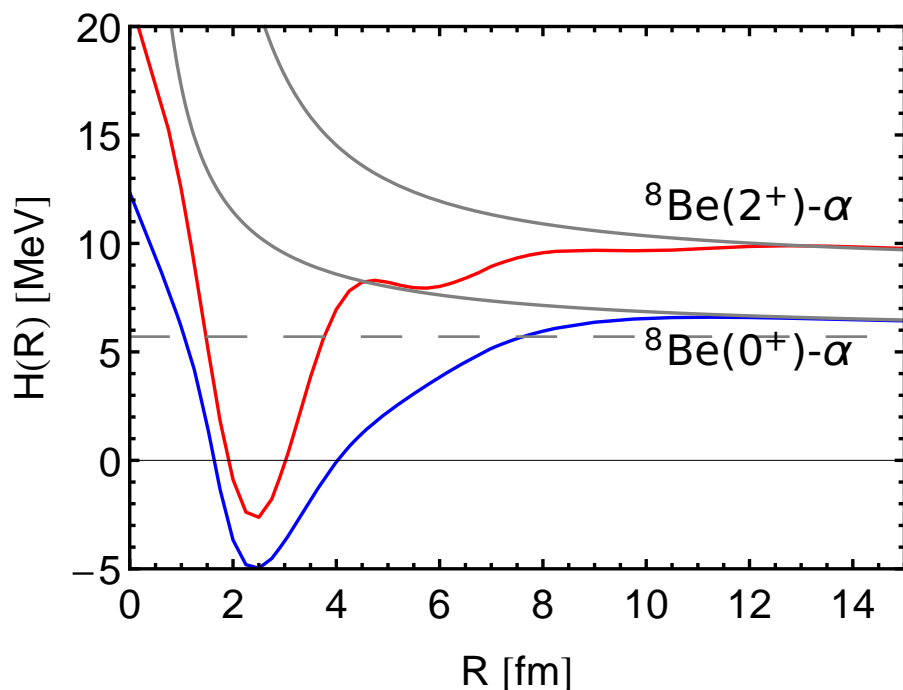
then the combined wave function

$$|\Psi_{IK;JM\pi}^{8\text{Be},4\text{He}}(R_j)\rangle = P_{\sim}^{\pi} P_{\sim MK}^J \mathcal{A} \left\{ |\Psi_{IK}^{8\text{Be}}(-\frac{R_j}{3}\mathbf{e}_z)\rangle \otimes |\Psi^{4\text{He}}(+\frac{2R_j}{3}\mathbf{e}_z)\rangle \right\}$$

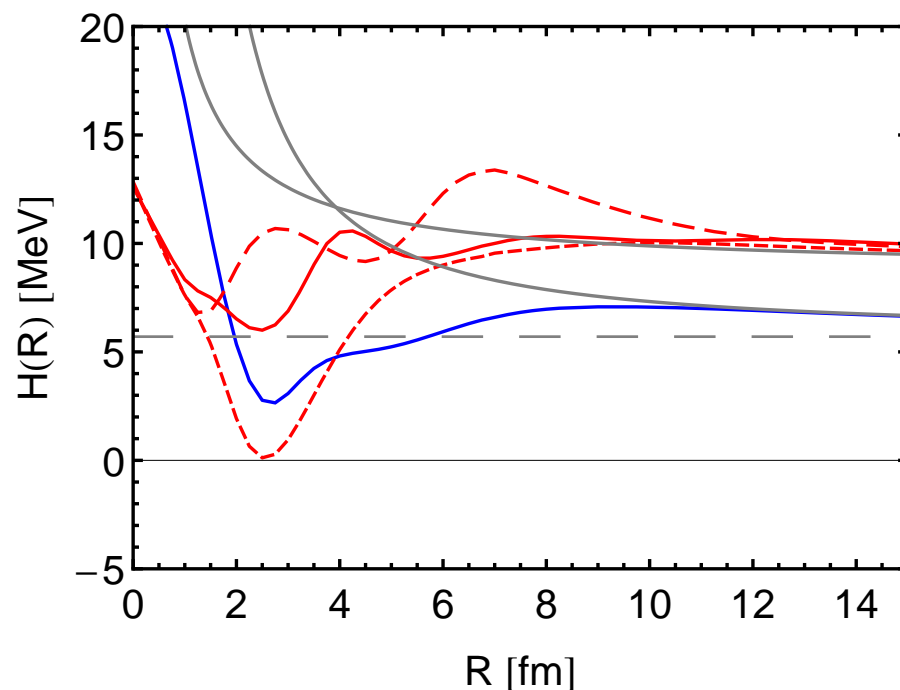
- will allow to match to Coulomb asymptotics

- Microscopic α -Cluster Model
- $^8\text{Be}-\alpha$ Energy Surfaces

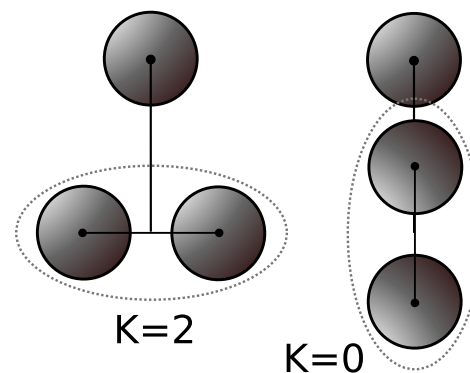
$J^\pi = 0^+$



$J^\pi = 2^+$



- energy surfaces contain localization energy for relative motion of ^8Be and α
- 2^+ energy surface depends strongly on orientation of ^8Be 2^+ state: $K=2$ most attractive



Microscopic α -Cluster Model

Bound state approximation – Convergence ?

	$\rho < 6$ fm	$\rho < 6$ fm, $R < 9$ fm	$\rho < 6$ fm, $R < 12$ fm	$\rho < 6$ fm, $R < 15$ fm	Experiment
$E(0_1^+)$	-89.63	-89.64	-89.64	-89.64	-92.16
$E^*(2_1^+)$	2.53	2.54	2.54	2.54	4.44
$E^*(0_2^+), \Gamma_\alpha(0_2^+)$	8.53	7.82	7.78	7.76	$7.65, (8.5 \pm 1.0)10^{-6}$
$E^*(2_2^+), \Gamma_\alpha(2_2^+)$	10.11	9.18	9.08	8.93	10.03(11), 0.80(13) [3]
$r_{\text{charge}}(0_1^+)$	2.53	2.53	2.53	2.53	2.47(2)
$r(0_1^+)$	2.39	2.39	2.39	2.39	–
$r(0_2^+)$	3.21	3.68	3.78	3.89	–
$B(E2, 2_1^+ \rightarrow 0_1^+)$	9.03	9.12	9.08	9.08	7.6(4)
$M(E0, 0_1^+ \rightarrow 0_2^+)$	7.20	6.55	6.40	6.27	5.47(9) [2]
$B(E2, 2_2^+ \rightarrow 0_1^+)$	3.65	2.48	2.09	1.33	0.73(13) [3]

- properties of resonances (Hoyle state and second 2^+ state) can not be determined in bound state approximation in an unambiguous way

[1] Ajzenberg-Selove, Nuc. Phys. **A506**, 1 (1990)

[2] Chernykh et al., Phys. Rev. Lett. **105**, 022501 (2010)

[3] Zimmermann et al., Phys. Rev. Lett. **110**, 152502 (2013); these numbers are under discussion

- Microscopic α -cluster model

- **Matching to Coulomb asymptotics**

Model Space

- Internal region: 3- α configurations on a grid
- External region: ${}^8\text{Be}(0^+, 2^+, 4^+)$ - α configurations
- Asymptotically: only Coulomb interaction between ${}^8\text{Be}$ and ${}^4\text{He}$ clusters

GCM basis state expressed in RGM basis

- Microscopic GCM wave functions are functions of single-particle coordinates: internal wave functions of cluster, the relative motion of the clusters and the total center-of-mass motion are entangled
- Write GCM basis state in external region with RGM basis states

$$|\Psi_{IK;JM\pi}^{8\text{Be},4\text{He}}(R_j)\rangle = \sum_L \left\langle \begin{matrix} I & L \\ K & 0 \end{matrix} \middle| \begin{matrix} J \\ K \end{matrix} \right\rangle \int drr^2 \Gamma_L(R_j; r) |\Phi_{(IL)JM\pi}^{8\text{Be},4\text{He}}(r)\rangle \otimes |\Phi^{\text{cm}}\rangle$$

with $(\pi = (-1)^L)$

$$\langle \boldsymbol{\rho}, \xi_a, \xi_b | \Phi_{(IL)JM\pi}^{8\text{Be},4\text{He}}(r) \rangle = \sum_{M_I, M_L} \left\langle \begin{matrix} I & L \\ M_I & M_L \end{matrix} \middle| \begin{matrix} J \\ M \end{matrix} \right\rangle \mathcal{A} \left\{ \frac{\delta(\rho - r)}{r^2} \Phi_{IM_I}^{8\text{Be}}(\xi_a) \Phi^{4\text{He}}(\xi_b) Y_{LM_L}(\hat{\rho}) \right\}$$

- asymptotically RGM states have good channel spin I and orbital angular momentum L

- Microscopic α -cluster model

- **Matching to Coulomb asymptotics**

RGM norm kernel and Overlap functions

- RGM norm kernel reflects effects of antisymmetrization, channel $c = (IL)J$

$$N_{c,c'}(r, r') = \langle \Phi_c(r) | \Phi_{c'}(r') \rangle \xrightarrow{r, r' \rightarrow \infty} \delta_{cc'} \frac{\delta(r - r')}{rr'}$$

- Overlap functions can be interpreted as wave functions for point-like clusters

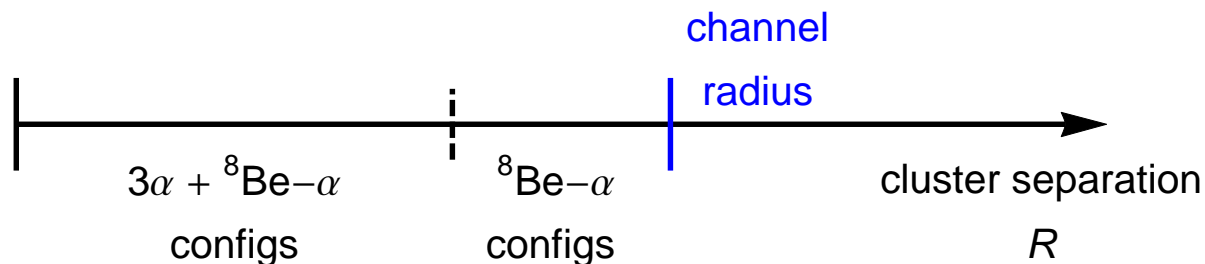
$$\psi_c(r) = \int dr' r'^2 N_{c,c'}^{-1/2}(r, r') \langle \Phi_{c'}(r') | \Psi \rangle$$

Matching to the asymptotic solution

- Use multichannel microscopic R -matrix approach

Descouvemont, Baye, Phys. Rept. 73, 036301 (2010)

- Check that results are independent from channel radius: used $a = 16.5$ fm here



- Microscopic α -cluster model
- Matching to Coulomb asymptotics

Bound states

- Whittaker functions

$$\psi_c(r) = A_c \frac{1}{r} W_{-\eta_c, L_c + 1/2}(2\kappa_c r), \quad \kappa_c = \sqrt{-2\mu(E - E_c)}$$

Resonances

- purely outgoing Coulomb, k complex

$$\psi_c(r) = A_c \frac{1}{r} O_{L_c}(\eta_c, k_c r), \quad k_c = \sqrt{2\mu(E - E_c)}$$

Scattering states

- in- and outgoing Coulomb (incoming channel c_0)

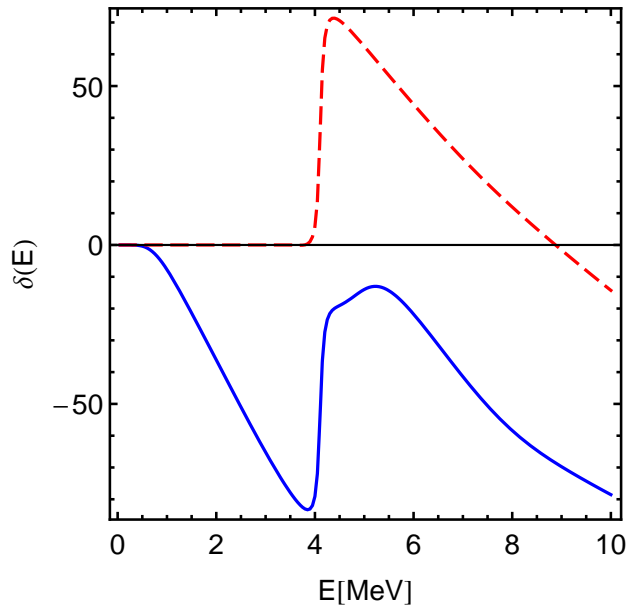
$$\psi_c(r) = \frac{1}{r} \{ \delta_{L_c, L_0} I_{L_c}(\eta_c, k_c r) - S_{c, c_0} O_{L_c}(\eta_c, k_c r) \}, \quad k_c = \sqrt{2\mu(E - E_c)}$$

- Diagonal phase shifts and inelasticity parameters: $S_{cc} = \eta_c \exp\{2i\delta_c\}$
- Eigenphases: $S = U^{-1} D U, D_{\alpha\alpha} = \exp\{2i\delta_\alpha\}$

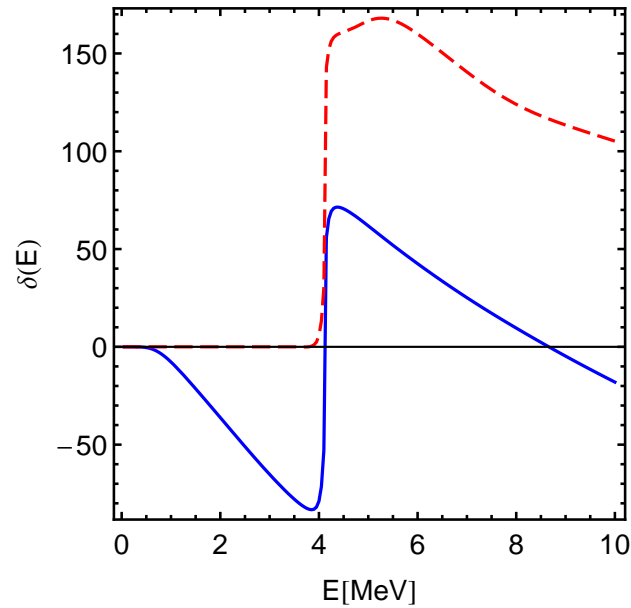
Cluster Model: ${}^8\text{Be}(0_1^+, 2_1^+)-\alpha$ Continuum

0^+ Phase shifts

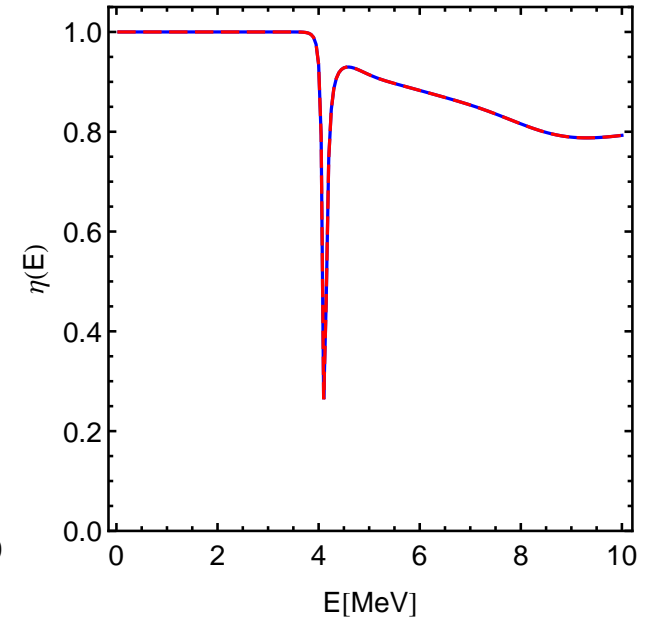
Eigenphaseshifts



Phaseshifts



Inelasticities



Gamow states

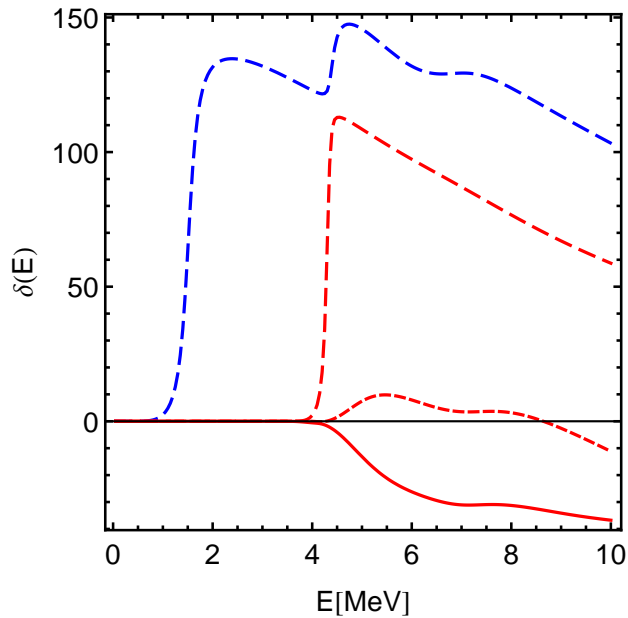
	E [MeV]	Γ_α [MeV]
0_2^+	0.29	$1.78 \cdot 10^{-5}$
0_3^+	4.11	0.12
0_4^+	4.76	1.57

- Hoyle state missed when scanning the phase shifts
- non-resonant background
- strong coupling between ${}^8\text{Be}(0^+)$ and ${}^8\text{Be}(2^+)$ channel at 4.1 MeV

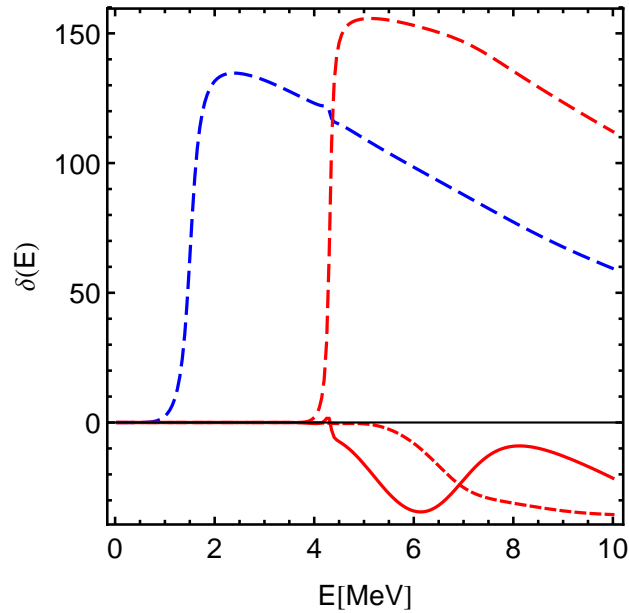
Cluster Model: ${}^8\text{Be}(0_1^+, 2_1^+)$ - α Continuum

2^+ Phase shifts

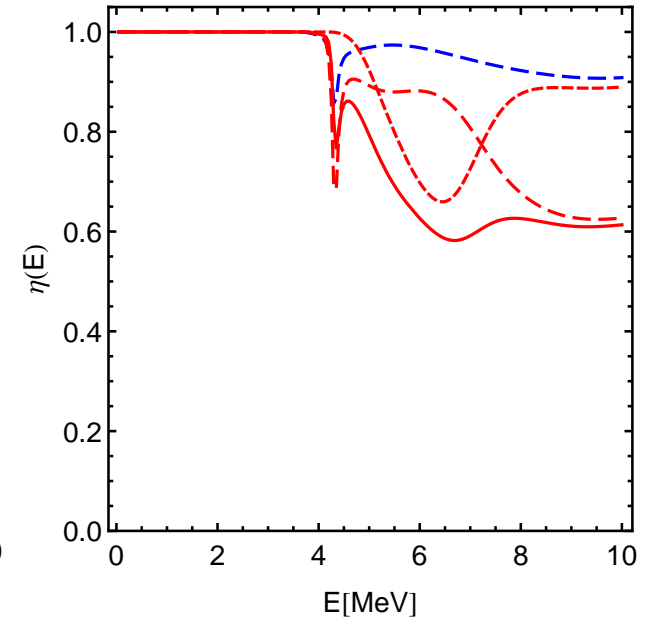
Eigenphaseshifts



Phaseshifts



Inelasticities



Gamow states

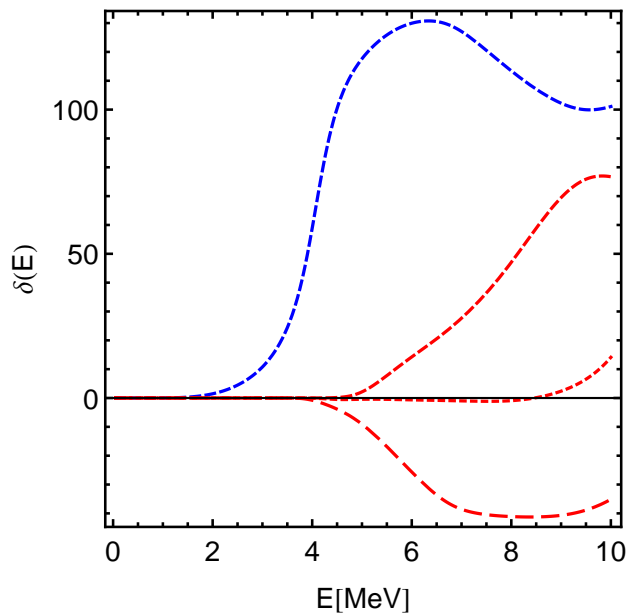
	E [MeV]	Γ_α [MeV]
2_2^+	1.51	0.32
2_3^+	4.31	0.14
...		

- non-resonant background
- $L = 2$ ${}^8\text{Be}(0^+)$ and ${}^8\text{Be}(2^+)$ resonances

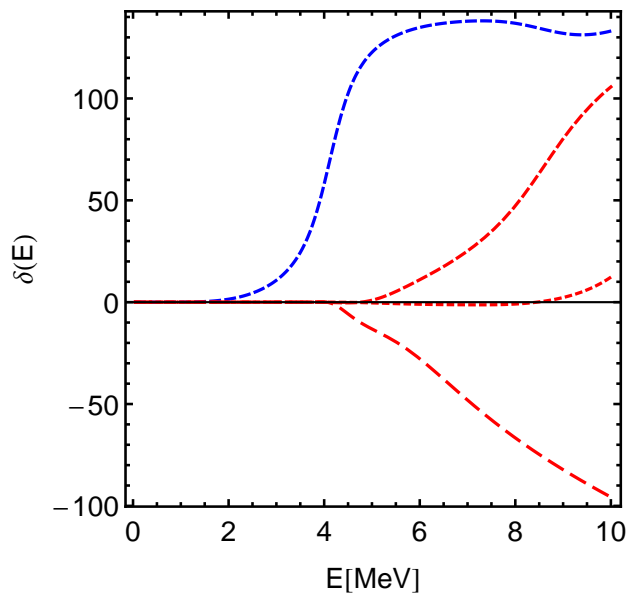
Cluster Model: ${}^8\text{Be}(0_1^+, 2_1^+)-\alpha$ Continuum

4⁺ Phase shifts

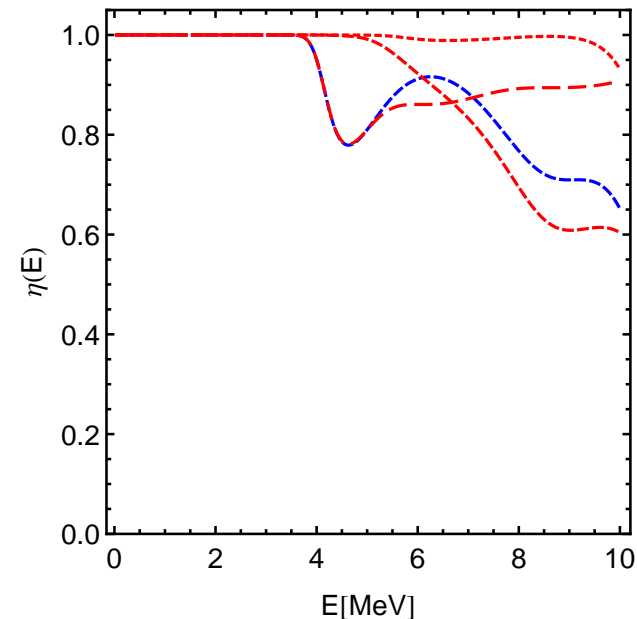
Eigenphaseshifts



Phaseshifts



Inelasticities



Gamow states

	E [MeV]	Γ_α [MeV]
4 ₁ ⁺	1.17	$8.07 \cdot 10^{-6}$
4 ₂ ⁺	4.06	0.98
...		

- 4₁ state (ground state band) very narrow, missed when scanning phase shifts
- 4₂⁺ state mostly ${}^8\text{Be}(0_1^+)$ but some mixing

Microscopic α -Cluster Model

Observables with proper treatment of Continuum

	$\rho < 6$ fm $R < 9$ fm	$\rho < 6$ fm $R < 12$ fm	$\rho < 6$ fm $R < 15$ fm	$\rho < 6$ fm Continuum	Experiment
$E(0_1^+)$	-89.64	-89.64	-89.64	-89.64	-92.16
$E^*(2_1^+)$	2.54	2.54	2.54	2.54	4.44
$E^*(0_2^+), \Gamma_\alpha(0_2^+)$	7.82	7.78	7.76	7.76, $3.04 \cdot 10^{-3}$	7.65, $(8.5 \pm 1.0) \cdot 10^{-6}$
$E^*(2_2^+), \Gamma_\alpha(2_2^+)$	9.18	9.08	8.93	8.98, 0.46	10.03(11), 0.80(13)
$r_{\text{charge}}(0_1^+)$	2.53	2.53	2.53	2.53	2.47(2)
$r(0_1^+)$	2.39	2.39	2.39	2.39	–
$r(0_2^+)$	3.68	3.78	3.89	$4.08 + 0.07i$	–
$B(E2, 2_1^+ \rightarrow 0_1^+)$	9.12	9.08	9.08	9.08	7.6(4)
$M(E0, 0_1^+ \rightarrow 0_2^+)$	6.55	6.40	6.27	$6.15 + 0.01i$	5.47(9)
$B(E2, 2_2^+ \rightarrow 0_1^+)$	2.48	2.09	1.33	$2.14 + 1.45i$	0.73(13)

- Resonances are calculated as Gamow states
- Matrix elements including resonances are regulated according to Berggren and Gyarmati
- Imaginary part provides information about uncertainty of matrix elements

Berggren, Nucl. Phys. **A109**, 265 (1968)

Gyarmati, Krisztinkovics, Vertse, Phys. Lett. **B41**, 475 (1972)

Berggren, Phys. Lett. **B373**, 1 (1996)

Work in Progress: FMD calculations with ^8Be - α continuum



UCOM interaction

- AV18 UCOM(SRG) ($\alpha=0.20 \text{ fm}^4$, $\lambda=1.5 \text{ fm}^{-1}$)
- Increase strength of spin-orbit force by a factor of two to partially account for omitted three-body forces

^8Be - α Continuum

- To get a good description of ^8Be it is essential to include polarized configurations
- ➔ Calculate strength distributions
- ➔ Investigate non-cluster states: non-natural parity states, $T = 1$ states, M1 transitions, ^{12}B and ^{12}N β -decay into ^{12}C , ...

Model space in internal region

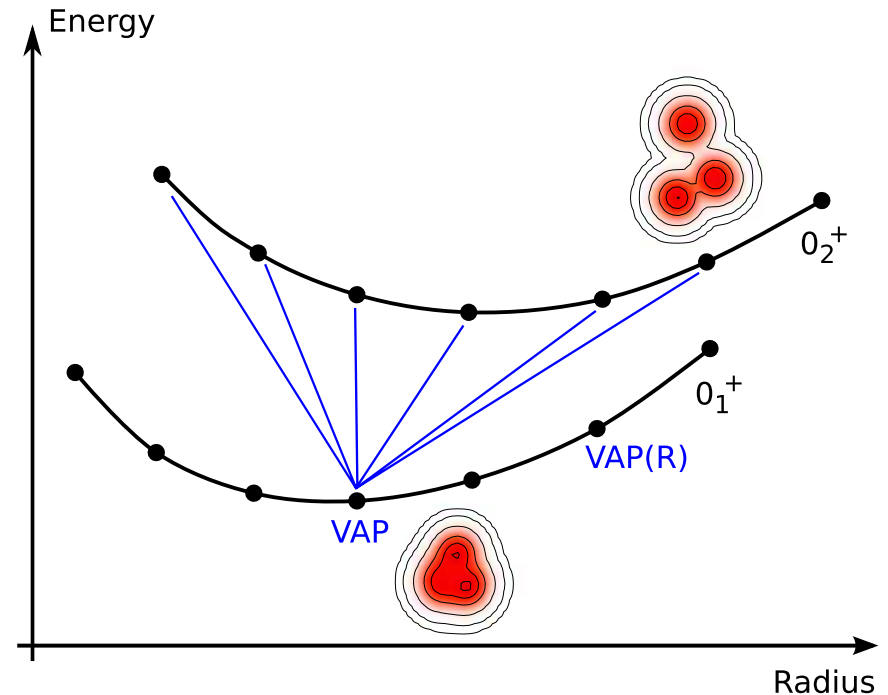
Model Space

- no assumption of α -clustering
- complete basis not feasible, find the “most important” basis states
- determine wave packet parameters by variation

VAP, VAP with constraints, Multiconfiguration-VAP

For each angular momentum (0^+ , 1^+ , 2^+ , ...)

- **VAP**: vary energy of projected Slater determinant $\tilde{P}^\pi \tilde{P}_{MK}^J |Q(q_i)\rangle$ with respect to all parameters q_i
- **VAP(R)**: create additional basis states by variation with a constraint on the radius of the intrinsic state
- **MC-VAP**: keep VAP state fix and vary the parameters of a second Slater determinant to minimize the energy of the second eigenstate in a multiconfiguration mixing calculation
- **MC-VAP(R)**: create additional basis states by adding a constraint on the radius of the second intrinsic state



FMD

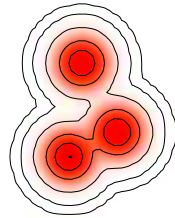
Important Configurations

- Calculate the overlap with FMD basis states to find the most important contributions to the eigenstates (in bound state approximation)

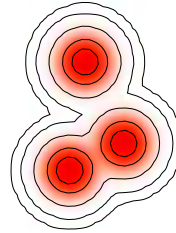


$$|\langle \cdot | 0_1^+ \rangle| = 0.94$$

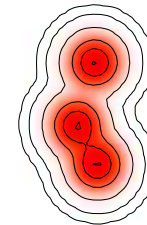
$$|\langle \cdot | 2_1^+ \rangle| = 0.93$$



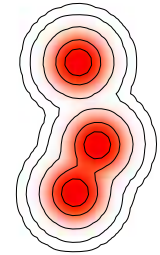
$$|\langle \cdot | 0_2^+ \rangle| = 0.64$$



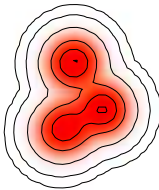
$$|\langle \cdot | 0_2^+ \rangle| = 0.58$$



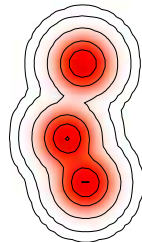
$$|\langle \cdot | 0_2^+ \rangle| = 0.57$$



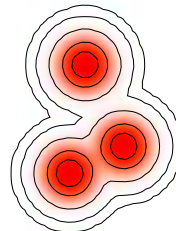
$$|\langle \cdot | 0_2^+ \rangle| = 0.45$$



$$|\langle \cdot | 3_1^- \rangle| = 0.91$$



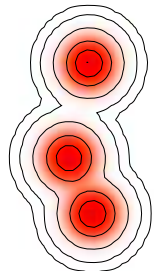
$$|\langle \cdot | 2_2^+ \rangle| = 0.50$$



$$|\langle \cdot | 2_2^+ \rangle| = 0.49$$



$$|\langle \cdot | 2_2^+ \rangle| = 0.44$$

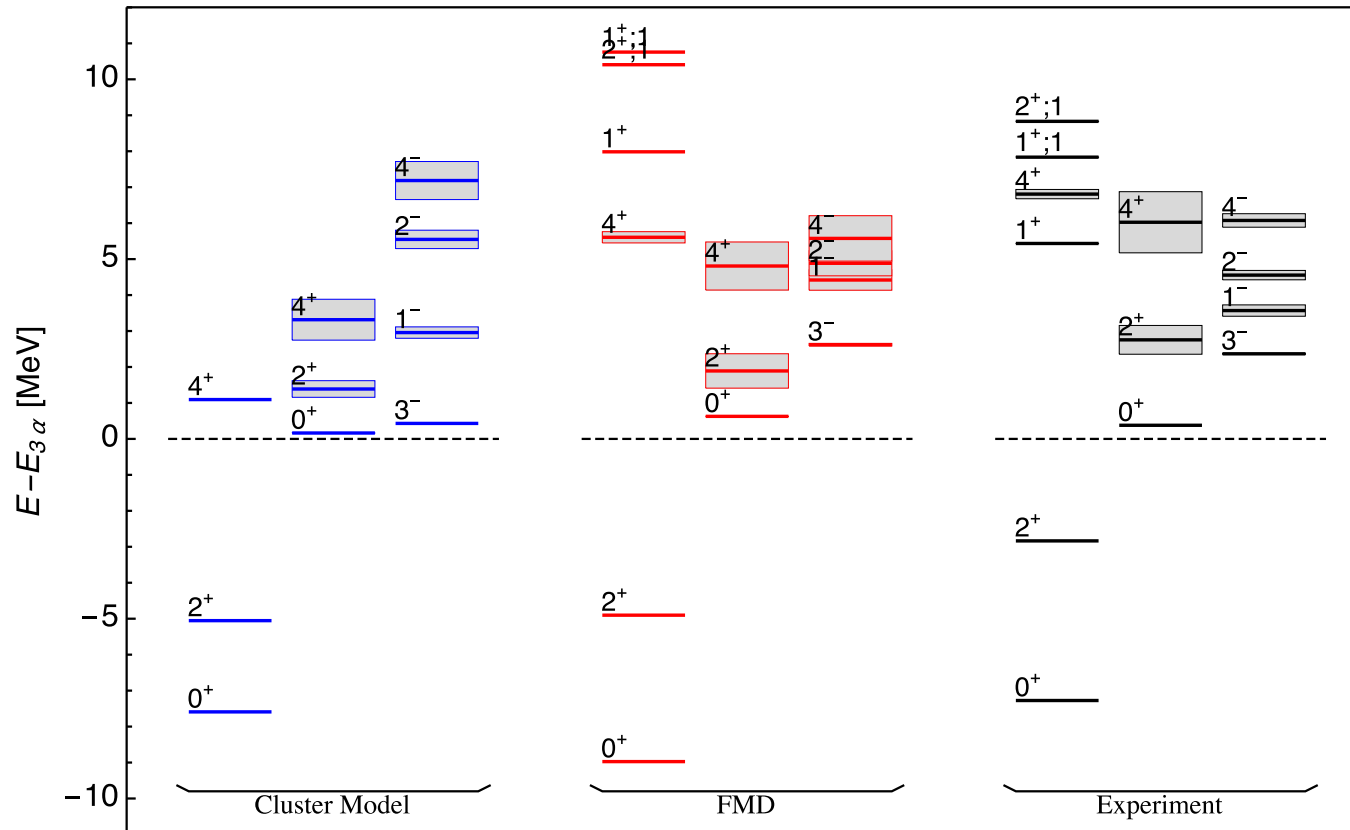


$$|\langle \cdot | 2_2^+ \rangle| = 0.41$$

FMD basis states are not orthogonal!

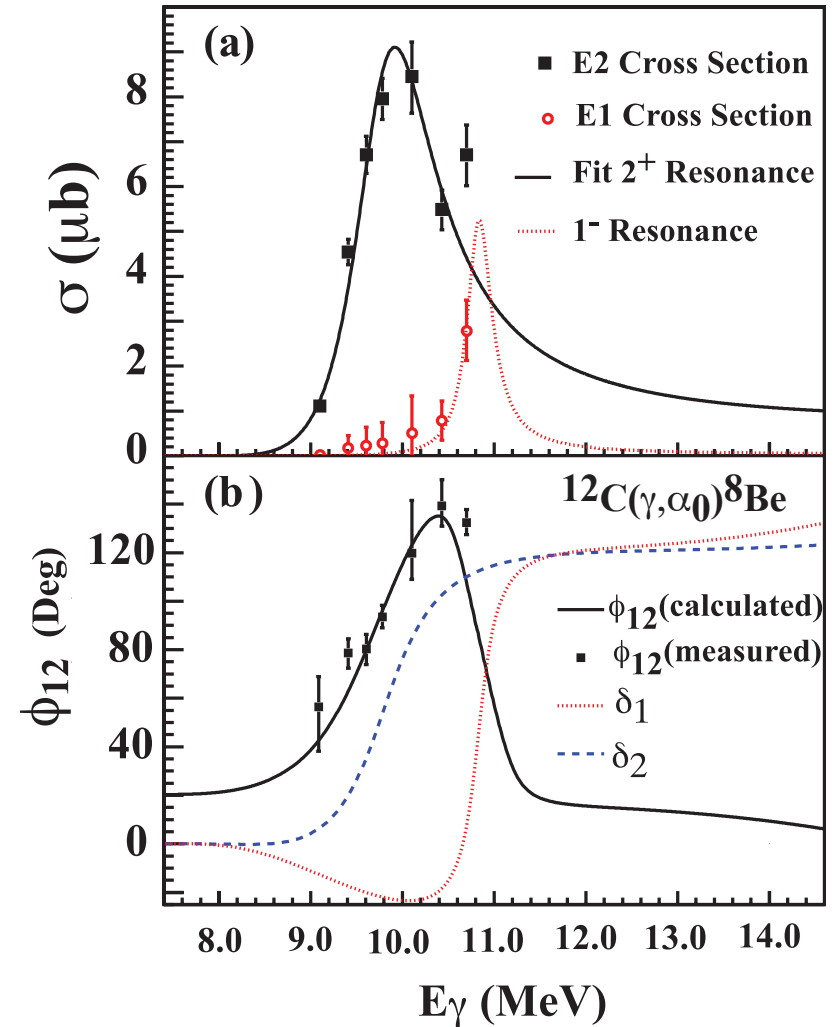
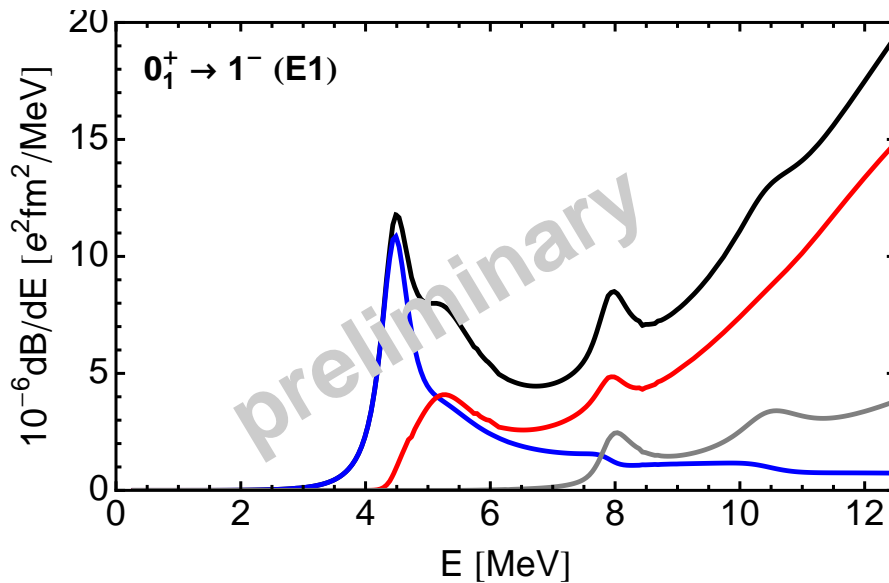
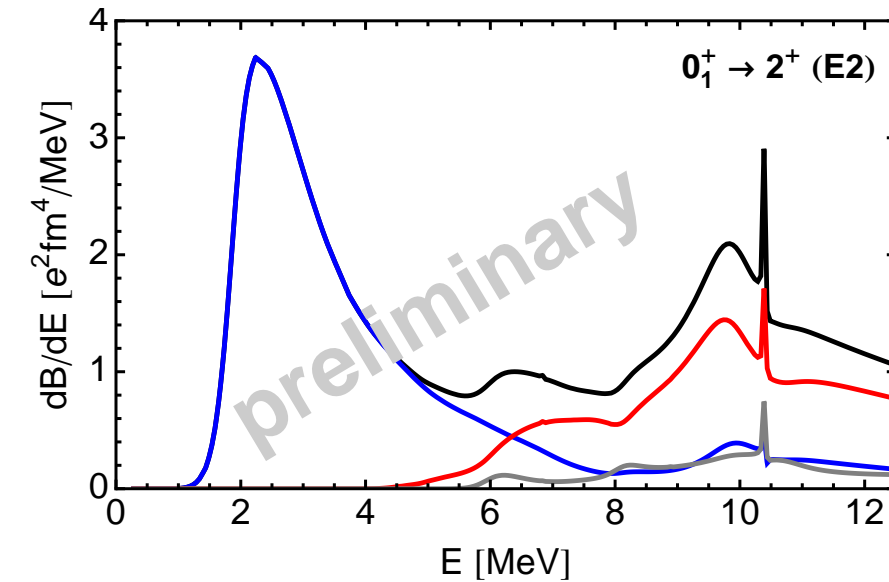
0_2^+ and 2_2^+ states have no rigid intrinsic structure

FMD/Cluster Model: $^8\text{Be}-\alpha$ Continuum Spectrum



- FMD describes the ground state band, the cluster states related to the Hoyle state and the negative parity states reasonably well
- Spin-flip states ($1^+ T = 0, 1$ and $2^+ T = 1$) are somewhat too high in energy

FMD: $^8\text{Be}-\alpha$ Continuum Strength distributions



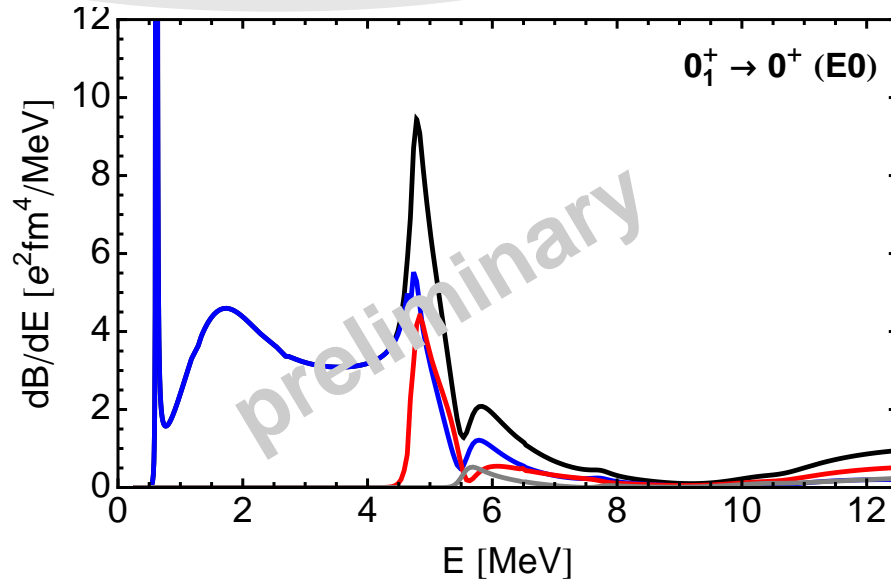
Zimmermann et al.,
Phys. Rev. Lett. **110**, 152502 (2013)

✗ E1 transition isospin-forbidden in cluster model !

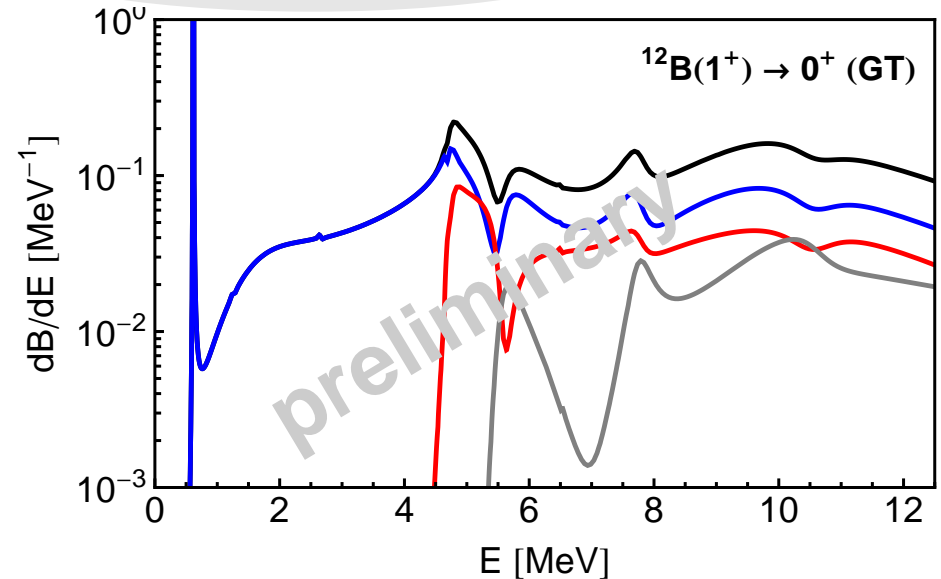
FMD: ^8Be - α Continuum

Population of 0^+ continuum with different reactions

Monopole response



β -decay

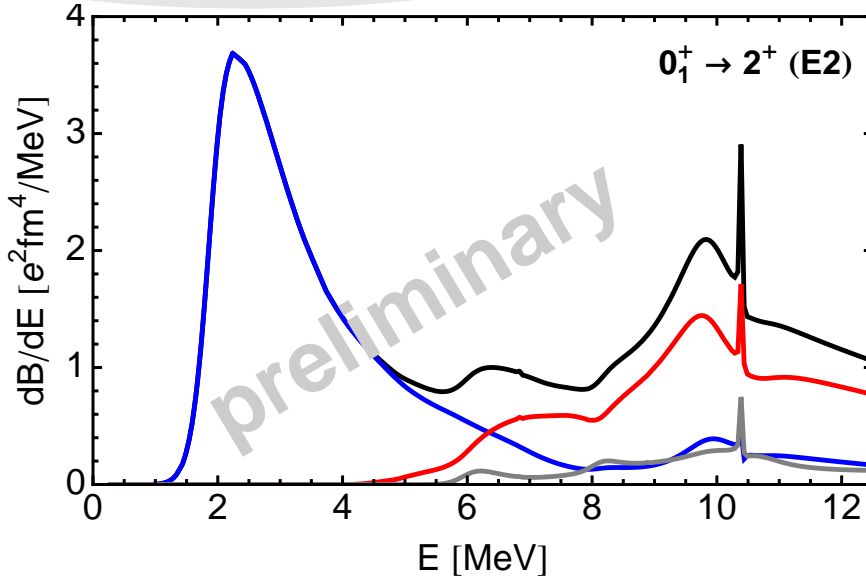


- GT transitions probe admixtures of “shell model” components
- Hoyle state populated in β -decay
- third 0^+ state decays through both $^8\text{Be}(0^+)$ - α and $^8\text{Be}(2^+)$ - α channels
– does this reflect a three-body resonance ?

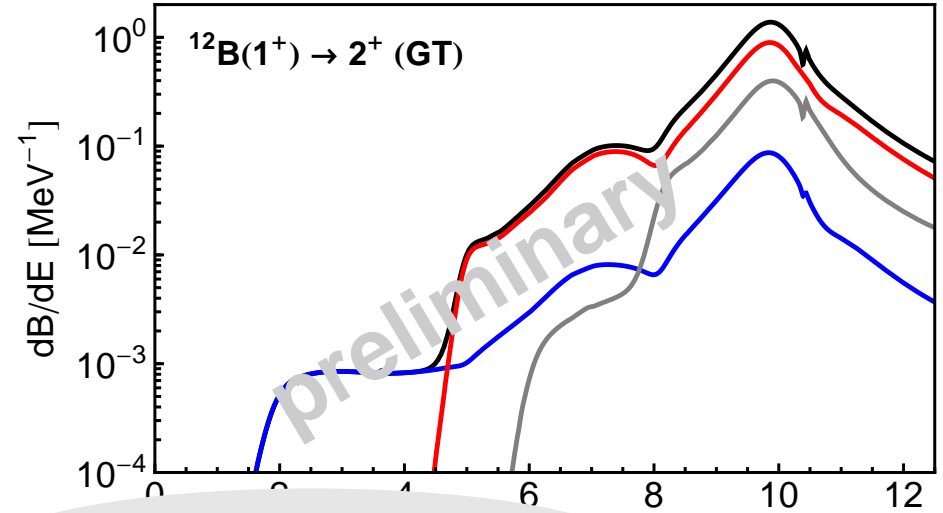
FMD: $^8\text{Be}-\alpha$ Continuum

Population of 2^+ continuum with different reactions

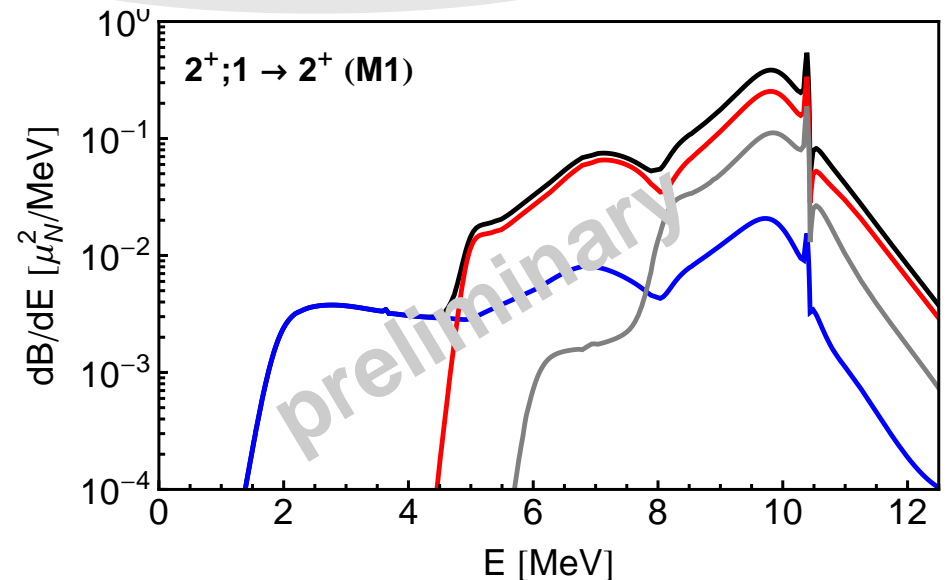
Quadrupole response



β -decay



M1 from $2^+(T=1)$



- 2_2^+ state very weakly populated in β -decay and in M1 transitions
- β -decay and M1 transitions from $2^+(T=1)$ state strongly populate 2^+ states that decay mainly through $^8\text{Be}(2^+)-\alpha$

Summary

Unitary Correlation Operator Method

- Explicit description of short-range central and tensor correlations

Fermionic Molecular Dynamics

- Gaussian wave-packet basis contains HO shell model and Brink-type cluster states

${}^3\text{He}(\alpha, \gamma){}^7\text{Be}$ Radiative Capture

- Bound states, scattering states, capture cross sections

Microscopic cluster model for ${}^{12}\text{C}$

- Model space with 3 α and ${}^8\text{Be}-\alpha$ configurations
- Matching with Coulomb continuum, resonances and scattering states
- Hoyle state band build on ${}^8\text{Be}(\text{gs})-\alpha$

FMD calculations for ${}^{12}\text{C}$

- VAP and Multiconfig-VAP in internal region, ${}^8\text{Be}-\alpha$ in external region
- Investigate EM and GT transitions to the continuum

➡ ${}^8\text{Be}-\alpha$ vs real three-body asymptotics ?